



(NASA-CR-152510) RADAR SYSTEMS FOR A POLAR MISSION, VOLUME 1 (Kansas Univ. Center for Research, Inc.) 89 p HC A05/EF 101 CSCL 08H

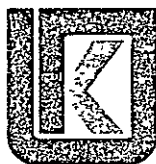
N77-23560

Unclas
G3/43 41347



THE UNIVERSITY OF KANSAS CENTER FOR RESEARCH, INC.

2291 Irving Hill Rd —Campus West Lawrence, Kansas 66044



THE UNIVERSITY OF KANSAS SPACE TECHNOLOGY CENTER
Raymond Nichols Hall

2291 Irving Hill Drive—Campus West Lawrence, Kansas 66045

Telephone:

RADAR SYSTEMS FOR A POLAR MISSION
FINAL REPORT

Remote Sensing Laboratory
RSL Technical Report 291-2
Volume I

R. K. Moore
J. P. Claassen
R. Erickson
R. K. T. Fong
M. Komen
J. McCauley
S. McMillan
S. K. Parashar

February, 1977

Supported by:

NATIONAL AERONAUTICS AND SPACE ADMINISTRATION
Goddard Space Flight Center
Greenbelt, Maryland 20771

CONTRACT NAS 5-22325

CRES



REMOTE SENSING LABORATORY

VOLUME I TABLE OF CONTENTS

LIST OF TABLES	iii
LIST OF FIGURES	iii
ABSTRACT	iv
1. INTRODUCTION	1
1.1.1 State of the Art - Monitoring of Sea Ice	3
1.1.2 State of the Art - Radar Monitoring of Icebergs	5
1.1.3 State of the Art - Radar Monitoring of Glaciers and Continental Ice	7
1.1.4 Mission Requirements	9
1.1.5 A Possible Scansar System for Polar Mission (based on SCANSAR for water resources mission).	10
1.1.5.1 Swath - Widening Techniques	11
1.1.5.2 Varying Pointing Angle.	11
1.1.5.3 Calibration of SAR.	12
1.1.5.4 The Scansar Concept	13
1.1.5.5 SAR System Components	16
1.1.6 SAR Processing Studies.	18
1.1.6.1 Multi-Look Unfocussed Synthetic Aperture.	21
1.1.6.2 Correlation Processor	24
1.1.6.3 Focussed Processor Using FFT Filtering.	27
1.1.6.4 Electronic Fresnel-Zone Plate Processor	30
1.1.6.5 CCD-SAW Processor Proposed at RRE	31
1.1.6.6 Range-Sequential Semifocussed Comb-Filter Processor	32
1.1.6.7 CCD Range-Sequential Synthetic Aperture Processor (TI/JPL).	36

1.2 Basic Conclusions	39
1.2.2 Recommendations	41
2. RADAR CAPABILITIES FOR THE POLAR MISSION	45
2.1 Radar Mapping of Sea Ice - State of the Art	45
2.2 Radar Mapping of Icebergs - State of the Art.	61
2.3 Radar Mapping of Glaciers - State of the Art.	66
3. MISSION REQUIREMENTS	73
3.1 Angle of Incidence Requirements	73
3.2 Coverage Requirements	74
3.3 Polarization Requirements	78
3.4 Resolution Requirements	79
REFERENCES	81

LIST OF TABLES

Table	3.1-1	Angle of Incidence Requirements for Polar Missions	73
	3.2-1	Coverage Requirements for Polar Missions	75
	3.2-2	Swath Widths Required for Repeat Coverage- Perfect Polar Orbit-Simplified Calculations	76
	3.2-3	Swath Widths Possible for One-Side Coverage	77
	3.3-1	Required Polarizations	79
	3.4-1	Required Resolutions	79

LIST OF FIGURES

Figure	1	Comb filter passbands showing carrier and its side-bands (zero phase shift).	34
	2	Comb filter passbands phase-shifted to account for Doppler shifting.	34
	3	A comb filter delay line.	34

ABSTRACT

Use of radar is indicated for observation of phenomena in the polar regions, particularly during the dark months. This report reviews the status of radar observation of sea ice (quasi-operational from aircraft), glaciers (little known), and icebergs (feasible but little research, and problems in discriminating icebergs from ships). Techniques for satellite observation are presented, with emphasis on use of a scanning synthetic-aperture radar (SCANSAR) of modest resolution to achieve the wide swathwidth required for frequently repeated coverage. Methods for processing SCANSAR data onboard the satellite were investigated, and some 5 methods appear feasible at the present time, although more research is needed. Use of CCD and SAW devices appears particularly promising in the achievement of low-power-consumption processors, but the rapid advancement of the digital art means that sampled-data analog processors using CCD and MOS devices must continually be compared with their digital competitors to determine which is best at the time a design decision must be made.

RADAR SYSTEMS FOR A POLAR MISSION

FINAL REPORT

by

R. K. Moore

J. P. Claassen

R. Erickson

R. K. T. Fong

M. Komen

J. McCauley

S. McMillan

S. K. Parashar

I. INTRODUCTION

This is the final report of a study of radars for polar mission at The University of Kansas for Goddard Spaceflight Center under Contract NAS 5-22325. Major elements of the study included determination of the state of the art for radar measurement of

Sea ice

Icebergs

Glaciers,

determination of the required spacecraft parameters, study of synthetic-aperture radar systems to meet these parametric requirements, and study of techniques for on-board processing of the radar signals into images.

Significant new concepts developed include the following:

Scanning synthetic-aperture radar (SCANSAR) to achieve wide-swath coverage;

Single-sideband radar;

Comb-filter range-sequential, range-offset processing.

The state of the art of radar measurement of sea ice, icebergs, and glaciers is outlined in the Program Summary and the remainder of the report; our knowledge about the measurement of sea ice is good from a

qualitative and far from a quantitative standpoint; the knowledge of the ability of radar to measure icebergs is primarily confined to what can be done with ship or shore radars; and the knowledge of ability to measure glaciers is quite limited. The feasibility of the immediate development of a spacecraft polar-mission SAR has been established. Numerous candidates for the on-board processor have been examined; while most are feasible, the optimum choice awaits more study.

This work was carried on in parallel with a study of radar systems for water-resources missions. Details of the measurement state of the art for water-resources observables are contained in a parallel report under that contract (KU RSL Technical Report 295-3, Contract NAS 5-22384). Of particular interest in connection with the polar mission is the study of monitoring of lake and river ice (KU RSL TM-291-4, Appendix D of TR 295-3). Most of the work on radar systems and processing is common to the two projects. The report is organized in such a way that many common elements are contained in common volumes, whereas the elements unique to each study are in separate volumes.

The program summary that follows is succinct and presented in bullet-chart form. The main report is more extended, but in many places represents a brief summary of material contained in the appendices. These appendices have all been issued as separate technical reports and memoranda throughout the course of the work, so the project monitors could become aware of developments as soon as they were complete, rather than waiting for the final report.

1.1.1 STATE OF THE ART - RADAR MONITORING OF SEA ICE

- The radar signal responds to both surface geometry and volumetric inhomogeneities in sea ice.
- Radar signal strength at 13.3 GHz and 16.5 GHz is approximately proportional to sea-ice thickness in May north of Point Barrow. Quantitative results for other conditions unknown.
- At 13.3 GHz (May-Point Barrow) an ambiguity exists between signal strength received from ice < 18 cm thick and ice of the order of 1 meter thick for vertical and horizontal polarizations.
- This ambiguity can be resolved by image interpretation because of difference in texture for images of the thin and thicker ice.
- This ambiguity does not exist for cross-polarized signals (transmit one polarization and receive the orthogonal one).
- Radar signal strength at 0.4 GHz is more ambiguous with respect to ice thickness. Multi-year ice in the 2-4 meter thickness range gives weaker return than first-year 1-2 meter thick ice for all polarizations.
- Radar images clearly show open water (leads and polynyas) and pressure ridges, as well as differences in ice type.
- The USSR (Arctic and Antarctic Research Institute of Leningrad) is apparently using the Toros (translation: ice ridge) radar operationally for ice mapping. This is a 16 GHz real-aperture SLAR.

- Although lake ice signals are different from those of sea ice, the operational test by NASA Lewis Research Center of a near-real-time Great Lakes ice mapping system has been successful, using a crude resolution 9 GHz real-aperture SLAR.
- The optimum angle of incidence for ice mapping is unknown. It should exceed 30° from nadir. Quantitative data extend to 60° , but many images that have been used include observations beyond 80° .
- The optimum frequency for monitoring sea ice is unknown. Frequencies in the 9-16 GHz region have been used successfully, and 0.4 GHz scatterometry is not so satisfactory. 1.2 and 9 GHz images have been collected together in a few cases, and 9 GHz seems better.
- Cross polarization seems better than either like polarization because the ambiguity involving very thin ice can be resolved without image interpretation of texture. If power limitations were to preclude use of cross polarization, either like polarization could be used.
- Required resolution for sea-ice observation is not known. Most measurements have been made with quite crude resolution (the APS-94C used for lake-ice and many sea-ice missions has 75 meter slant-range resolution and 7.5 m along-track resolution [300 m at 40 km]); but the few images produced with finer resolution show features of interest not seen on the coarser-resolution images. Experimentation is needed.

1.1.2 STATE OF THE ART - RADAR MONITORING OF ICEBERGS

- Radar can be used successfully to detect icebergs.
- Most existing observations with ship or shore PPI radars (poor resolution, near-grazing incidence).
- Some SLAR observations - Lewis RC APS-94C poor resolution 9 GHz; USSR Arctic & Antarctic Institute Toros modest resolution 16 GHz.
- Biggest problem with systems used - distinguishing bergs from ships and large floes (separated pack ice).
- Reports on difficulty in distinguishing icebergs may be due to poor resolution, polarization, frequency, or angle of incidence.
- Bergs easiest to spot in dense pack ice or in open sea.
- Optimum frequency unknown - no research on this to date.
- Optimum angle of incidence unknown - no research on this to date. Angles away from vertical should be better because of contrast improvement relative to sea or pack ice.
- Optimum polarization unknown - no research on this to date. Horizontal or cross polarization should give better contrast with sea.
- Optimum resolution unknown - no research on this to date. Fine resolution should permit better distinction of shape relative to that of ships.

- Research needed to determine best frequency, polarization, angle of incidence, and resolution. Both quantitative research with spectrometer and use of fine-resolution images needed.

1.1.3 STATE OF THE ART - RADAR MONITORING OF GLACIERS AND CONTINENTAL ICE

- Glaciers have been observed with imaging radars, but almost never under controlled conditions.
- Both glacial margins and internal features (low lines, crevasses, etc.) have been seen.
- Firn, important in glacial boundaries and as an early stage in glacial ice formation, has been observed on 35 GHz radar.
- Glacial margins and features have been observed through cover of dry snow by radar under conditions that would have precluded identification using sensors in visible and IR region.
- The optimum frequency for radar observation of glaciers is unknown. The frequency may vary depending upon the phenomena to be observed, as indicated qualitatively in results to date.
- The optimum angle of incidence for radar observation of glaciers is unknown. In some mountainous settings this may be dictated by topography.
- The optimum polarization for radar observation of glaciers is unknown.
- The required resolution for radar observation of different glacial features is unknown.

- Research is required to determine both the capabilities and the optimum parameters for radar observation of glaciers. Such research should involve in situ observation with a microwave spectrometer and a consistent set of observations with a fine-resolution radar imager (preferably multi-frequency) accompanied by ground truth.

1.1.4 MISSION REQUIREMENTS

Application	Frequency of Coverage	Angle of Incidence	Desired Swath* (ideal orbit- 2 passes/orbit)	Polarization	Frequency (GHz)
-------------	-----------------------	--------------------	--	--------------	--------------------

Sea Ice General ice motion Navigation	2-10 days 1-3 days	{ >22° Min Max TBD }	416-83 km	VH or HV VH or HV	TBD (9-17 works) TBD (9-17 works)
Icebergs	1-3 days	{ >22° Min Max TBD }	831-277 km	HH (TBD)	TBD
Glaciers	6 months	TBD Will vary Between flat and mountain- ous terrain	831-277 km	TBD	TBD

Note: Where TBD (to be determined) is shown, insufficient information available to specify requirements.

*Simplified calculation assumes coverage on ascending and descending passes can be made non-overlapping with each other and with succeeding orbits.

1.1.5 A POSSIBLE SCANSAR SYSTEM FOR POLAR MISSION
(based on SCANSAR for water resources mission)

- Technology exists for developing SARs to meet all known water resources mission requirements with on-board processing except single-spacecraft 1-3 day repetition
- Required swath for frequent repetition exceeds that possible with standard SAR techniques
- Wider swath can be achieved with several techniques
- Scanning SAR (SCANSAR) appears most feasible swath-widening technique for modest-resolution small-spacecraft missions
- Techniques exist for pointing SAR on demand, but they increase complexity
- Space-qualified transmitter tubes are scarce, but techniques for building them are known.

1.1.5.1 SWATH - WIDENING TECHNIQUES

- Scanning SAR uses less power than other methods at sacrifice in resolution
- Swath may be doubled without scanning by alternating phase on successive pairs of pulses, but more power required and clutter noise increased
- Swath may be widened by transmitting on different, nearby, frequencies. In effect, each frequency requires a separate radar, but a common antenna may be used
- Outer subswaths require narrower vertical beams to overcome ambiguity, so antennas should be constructed to permit different beam widths
- Multiple separate antennas may also be used to overcome ambiguity problems

1.1.5.2 VARYING POINTING ANGLE

- Mechanical or electronic scan may be used
- For rare events like flood monitoring, changing spacecraft attitude may be better
- Large enough vertical aperture required to overcome ambiguity at largest expected incidence angle. Only part would be used for normal applications
- PRF and processing must be programmable if pointing angle to be varied

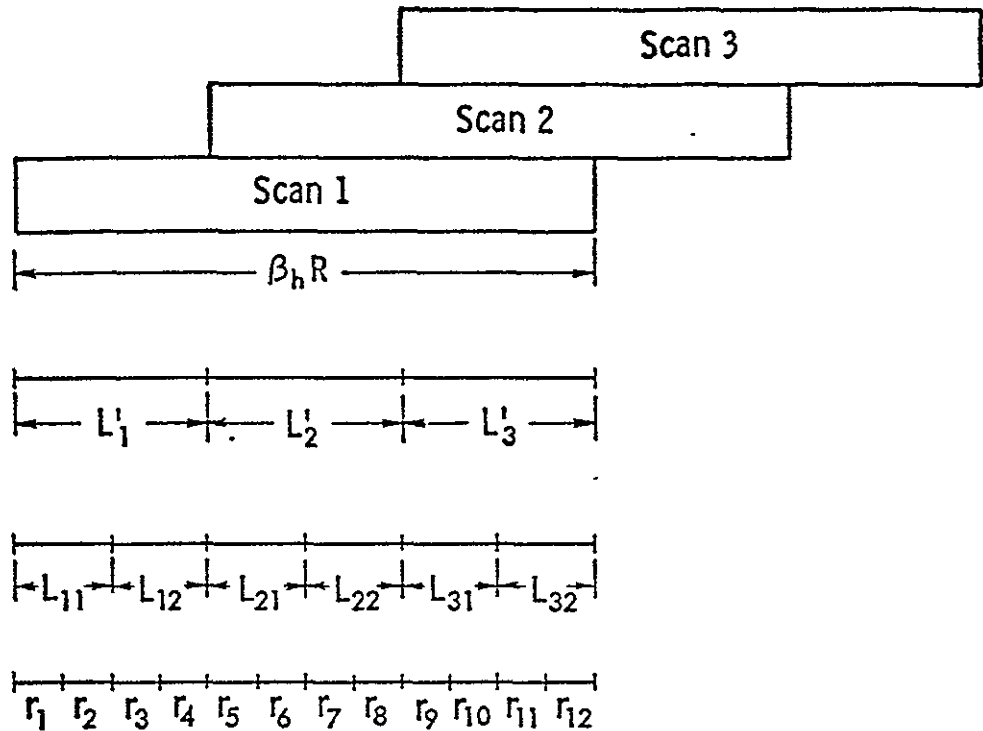
1.1.5.3 CALIBRATION OF SAR

- Only a few attempts have been made to calibrate SAR in the past, but these were reported successful
- Absolute calibration is difficult because antenna absolute gain measurements are difficult, particularly if antenna must be erected in space
- Quantity to be determined is ratio of receiver output voltage (or power) to transmitter power
- One method is to monitor transmitter peak or average power and receiver-processor transfer function separately. In this case a test signal is periodically generated and sent through receiver
- Better method is to make receiver-test signal proportional to transmitter power
- Best approach seems to be slaving amplitude of noise source to transmitter power level and transmitting the noise through receiver
- Another method slaves a test signal chirped like signal from a point target to the transmitter power
- In all practical systems transmitter power should be measured as close to antenna as possible and test signal injected as close to antenna as possible

1.1.5.4 THE SCANSAR CONCEPT

- SCANSAR (Scanning Synthetic Aperture Radar) seems best approach for wide-swath modest-resolution system
- SCANSAR uses step-scanned beam with each position having swath width limited by ambiguity, but combination not so limited
- SCANSAR involves compromise between swath width and resolution
- With SCANSAR, antenna length need not be long as in wide single-swath system. Area of antenna is fixed, but length/height ratio may be adjusted
- Usual compromise between azimuth resolution and number of independent samples averaged exists, but number of samples averaged is reduced by number of beam positions used
- Same processor can be used for each beam position, so total processor size small compared with achieving same coverage with single beam
- SCANSAR best understood by an example

SCANSAR EXAMPLE



- 3 beam positions
- 2 looks per beam position
- Azimuth resolution improvement over real aperture: 12
- Total distance available for building a synthetic aperture: $\beta_h R$
- Total distance available for building synthetic aperture for 1 scan position: L'
- Distance used for one synthetic aperture (1 look): L
- Azimuth resolution: r
- During each distance L processing necessary for all 12 r 's within beam at that time
- End effects neglected here
- Since only $1/6$ of potential aperture used for each look, potential resolution without scanning would be $r/6$; i.e., 72 cells could be imaged. Real aperture in this case is $r/3$

RECOMMENDED SCANSAR SYSTEM FOR WATER
RESOURCES MISSION

④ Frequency:	4.75 GHz
④ Coverage (angle from nadir):	7°-22°, 22°-37°
④ Azimuth Resolution:	50 to 53 m (inner swath) 50 to 57 m (outer swath)
④ Range Resolution	150 to 62 m (inner swath) 50 to 33 m (outer swath)
④ Spacecraft Altitude:	435 km
④ Antenna Size:	3m long by 1.07 m high
④ Independent Looks:	6 (inner swath) 3 (outer swath)
④ Beam Positions:	5 (inner swath) 10 (outer swath)
④ Swath Width:	122 km (inner); 124 km (inner, spherical earth) 150 km (outer); 157 km (outer, spherical earth)
④ Transmitter Peak Power:	142 watts
④ Transmitter Av. Power:	15 watts
④ Pulse Compression:	100:1
④ Bus Bar Power:	197 watts
④ Telemetry Rate:	3.85 Mb/s

All calculations based on plane-earth geometry. Minor modifications for spherical-earth geometry do not affect conclusions.

1.1.5.5 SAR SYSTEM COMPONENTS

- Both array and reflector antennas have been flown in space for many years. The technology is well advanced
- Electronically scanned antennas have been flown in space
- Mechanisms for successfully erecting large antennas in space have flown successfully
- Traveling-wave tubes (TWTs) with peak power in the 2 kW range have flown in space in the 13-14 GHz range. Scaling to lower frequencies should be easy
- Average powers as high as 100 watts have been reported for communication satellite applications
- Solid-state amplifiers are available with adequate power at L-band and probably at S-band. The state of this art is advancing rapidly upward in both power and frequency
- Non-cryogenic parametric amplifiers have been reported with noise figures from 0.36 dB at L-band to 1.23 dB at 20 GHz
- Noise figures for TDAs are in the 4.5-6.5 dB range between 1 and 20 GHz
- Noise figures are rapidly improving for both bipolar and FET transistor preamplifiers. 3.5-5 dB can be achieved with FETs in the 6-18 GHz range

- Below 6 GHz bipolar transistor amplifiers have good noise figures.
A 1.7 dB figure has been quoted at L-band
- Mixer-amplifier (IF) front ends can now be obtained in the 4-8 dB
noise figure range

1.1.6 SAR PROCESSING STUDIES

- Processing studies have concentrated on systems to work aboard the spacecraft
- Range compression is desirable and probably required in view of the transmitter state of the art
- Single-sideband transmission and processing appear to offer power savings of a factor of 2 in the transmitter and possibly in the processor. This new technique for radar needs further research before it can be applied to ambiguity-limited SAR
- Multiple-look processing permits use of much poorer azimuth resolution than possible with single-look processing. A theoretical basis has been established for evaluating the multi-look-resolution tradeoff
- Processor complexity for each look decreases inversely as the square of the azimuth resolution, so the maximum resolution feasible should be used
- Effective resolution for interpretability is determined by the area of the pixel, so trades may be made between range and azimuth resolution. Improving either resolution costs power, so no general statement can be made as to the best compromise between range and azimuth resolution
- Multi-look unfocussed processing is much simpler than focussed processing, and resolutions attainable at lower spacecraft altitudes may permit its use

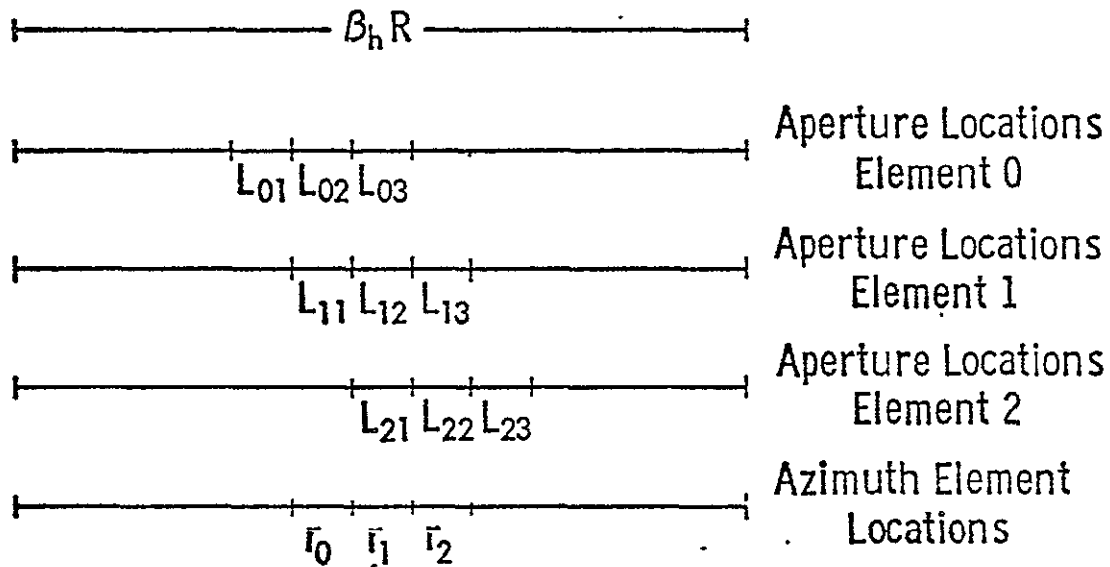
- Most previous designs for synthetic-aperture electronic processors operate on range-gated video, one range and azimuth element at a time
- Much effort here has been devoted to range-sequential rather than range-gated processors, since this method offers potential hardware and power savings (not necessarily realized in our early designs)
- Analog storage elements (CCD and serial analog memory -- SAM) appear to offer many advantages over digital techniques for some types of processors
- Use of SAM devices in comb filters (range-sequential processing) has been investigated in detail for the proposed SCANSAR
- Range-gated processors investigated include the following:
 - + Multi-look unfocussed processor
 - + Correlation processor (1975 review of spacecraft radar processor proposed at Kansas by Gerchberg in 1970 doctoral dissertation)
 - + Focussed processor using FFT
 - + Electronic-Fresnel-Zone Plate processor proposed at Kansas in 1965
 - + CCD-SAW (surface acoustic wave) processor proposed at Royal Radar Establishment in 1975
- Range-sequential processors investigated include the following:
 - + Comb-filter unfocussed processor using SAM devices
 - + Comb-filter semifocussed processor using SAM devices and

tunable filters

- + Comb-filter semifocussed processor using SAM devices and fixed filters (recommended for SCANSAR)
- + Texas Instruments - JPL CCD synthetic-aperture processor

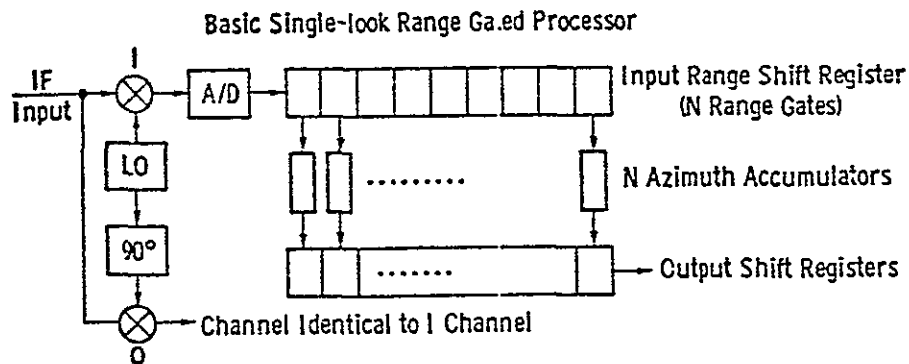
1.1.6.1 MULTI-LOOK UNFOCUSSED SYNTHETIC APERTURE

- Example shows 3 elements for a 3-look processor
- Resolution length = aperture length $L = \sqrt{\frac{\lambda R}{2}}$

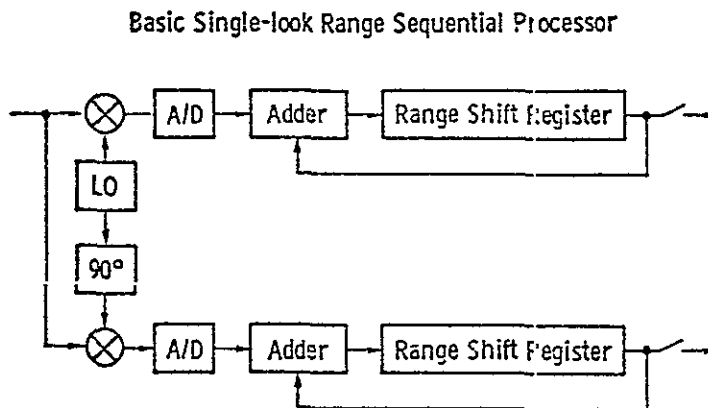


- Only a small part of potential aperture ($\beta_h R$) is used for each look
- In this example each aperture is 1/9 potential aperture; therefore 9 looks would be possible instead of the three shown
- Normal sideviewed elements are r_0 for L_{02} , r_1 for L_{12} , r_2 for L_{22}
- If only a single look for each element, a single simple processor is required; in this case 3 such processors are required
- Either range-gated or range-sequential (comb-filter processors may be used.

MULTI-LOOK UNFOCUSSED SYNTHETIC APERTURE (CONTINUED)



Input range shift register filled with each pulse and then transferred to azimuth accumulators. Output shift registers filled each aperture.



Contents of range shift register is shifted out and recirculated after adding to each incoming pulse; at end of an aperture the register contents are shifted out and the feedback loop is inhibited.

This processor could also be implemented without the A/D converters using SAM or CCD shift registers.

- Processor I and Q outputs are combined appropriately by taking square root of the sum of their squares

EXAMPLE:

SCANSAR

Spacecraft altitude:	435 km
Frequency:	4.75 GHz
Swath:	122 near swath 152 far swath

MULTI-LOOK UNFOCUSSED SYNTHETIC APERTURE (CONTINUED)

Cross-track resolution:	150 m near swath 50 m far swath
Range of Nadir Angles	7° - 22°, 22° - 37°
Power Consumption:	64 Watts (both sides)
Along-track resolution:	117 m (7°) to 131 m (37°)

1.1.6.2 CORRELATION PROCESSOR

- One way to view synthetic-aperture processing is correlation with a replica of the return signal from a point target, including especially the phase (and therefore frequency) variation
- The correlation processor is a range-gated processor
- The figure illustrates the operations for an input in the form of a range-gated bipolar video signal
- Separate channels identical to the one shown in the figure must be provided for each range element and for each azimuth element being processed at a single instant (see diagram for SCANSAR example; there 12 cells are processed simultaneously and the processor may be reused for each look and beam position, so the number of processors is 12 x (number of range elements))

EXAMPLE (SCANSAR)

Spacecraft Altitude:	435 km
Ground Velocity:	7.2 km/s
Carrier Wavelength:	6.3 cm
Real Aperture Length:	3 m
Range of Nadir Angles:	7° - 22° (near swath) 22° - 37° (far swath)
Swath Width:	122.3 km (near swath) 152 km (far swath)
Number of Looks Averaged:	6 (near swath) 3 (far swath)
Number of Scan Cells:	5 (near swath) 10 (far swath)

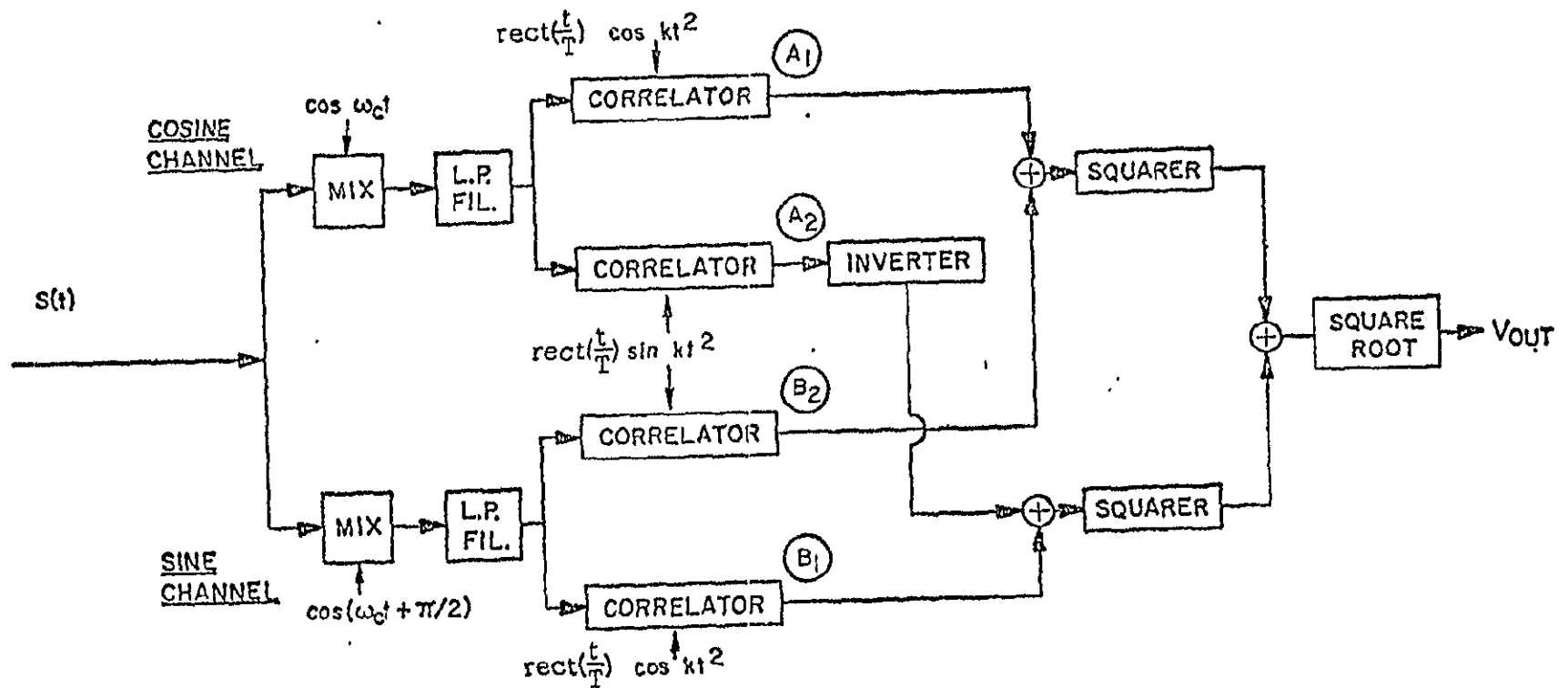
Range Resolution:	150-63 m (near swath) 50 m (far swath)
Azimuth Resolution:	39.5 - 49 m
Power Consumption (both sides):	170 watts

EXAMPLE (Updated Gerchberg processor)

Satellite altitude:	900 km		
Frequency:	10 GHz		
Antenna length:	8 m		
Square pixel size: (slant range res. = azimuth res.)	20 m	50 m	100 m
Number of subapertures: (independent samples)	5	12.5	25
Swath width (2 sides):	400 km		
Power required:	650 W	104 W	26 W

This example assumes the processor designed by Gerchberg (1970) with 1975 components. The power consumptions shown may vary from real requirements. However they illustrate the relation of power consumption to resolution.

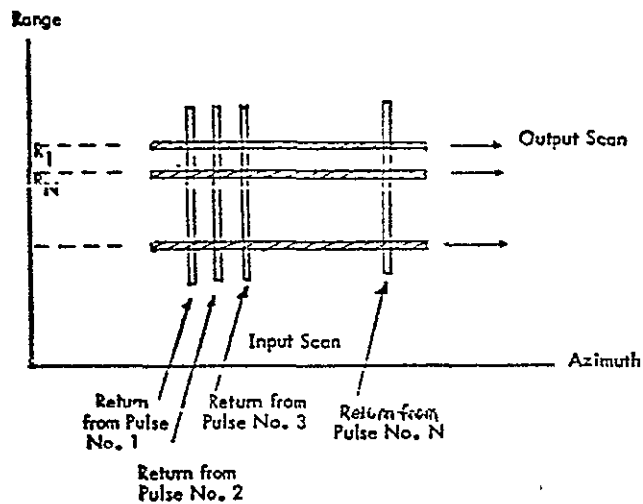
Algorithm Employed With Quadrature Detection *



* Gerchberg processor.

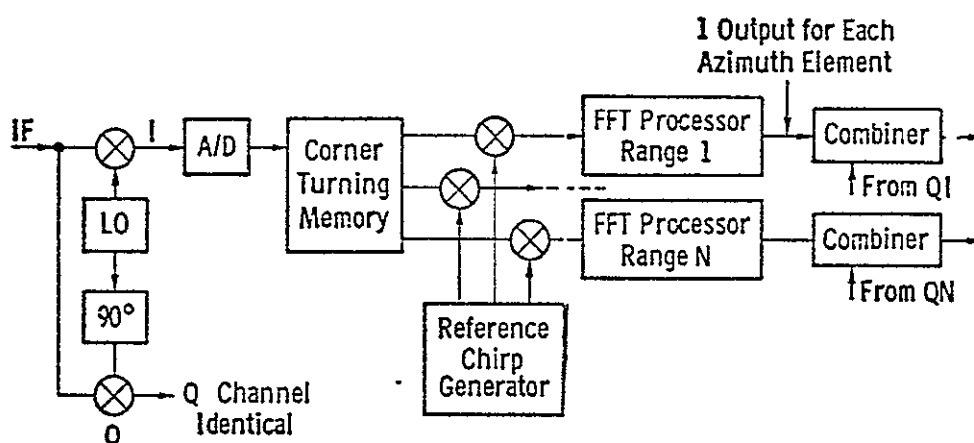
1.1.6.3 FOCUSED PROCESSOR USING FFT FILTERING

- This is a range-gated processor
- Methods for implementing the FFT are discussed in TM 295-9 (Appendix L)
- This type of processor has been constructed for various military aircraft radars
- A major part of this processor (and the other range-gated processors) is the "corner-turning memory" -- principle illustrated below:



- Since the corner-turning memory must contain all azimuth and range elements (samples) required to produce a synthetic aperture for each range, it can be very large; its size is inversely proportional to the cube of resolution for square pixels, so the advantage in processing for modest resolution is very great.
- Basic elements of the system are shown below:

FOCUSSED PROCESSOR USING FFT FILTERING (CONTINUED)



- Numerous other implementations are possible but all contain same elements; for example, I and Q outputs can be combined as complex numbers in the corner-turning memory and multiplied by complex numbers from the reference chirp generator
- Reference chirps for different ranges are different unless depth of focus is very large

EXAMPLE:

Spacecraft altitude:	435 km
Frequency:	4.75 GHz
Antenna length:	3 meters
Swath width:	122 km, 152 km (using SCANSAR technique)
Range of nadir angle:	7°-22°, 22°-37° (both sides)
Range resolution:	150 m (ground) at 7°, 50 m from 22°-37°
Number of beam positions:	5 (7°-22°), 10 (22°-37°)
Number of subapertures (independent looks):	6, 3
Power required:	90 Watts

1.1.6.4 ELECTRONIC FRESNEL-ZONE PLATE PROCESSOR

- A Fresnel-zone plate in optics has dark bands (zero transmission) in regions of a plane that would contribute to destructive interference. Illumination with a collimated beam results in focussing at a point.
- A synthetic-aperture analog of the Fresnel-zone plate was first proposed in 1965 by Moore and Buchanan at Kansas; this system has been examined in considerable detail here
- The Fresnel-zone-plate processor inverts rather than eliminates out-of-phase wave components, so they add in phase
- Implementation of the electronic Fresnel-zone-plate processor is similar to implementation of an unfocussed processor, except for a programmed premultiplication by ± 1 and the need for more processors because the synthetic aperture is longer. This simplicity of implementation was the reason for studying this approach
- Straightforward implementation of the EFZP processor results in large sidelobes for modest-resolution, short synthetic-aperture systems, but the sidelobes are more reasonable for longer apertures
- Weighting the signals from the outer edges of the aperture improves sidelobes if the weights are stronger than at the center (opposite to normal antennas)
- Because of the high sidelobes in the modest-resolution systems needed for the water resources mission, the EFZP processor in the forms studied does not seem meritorious

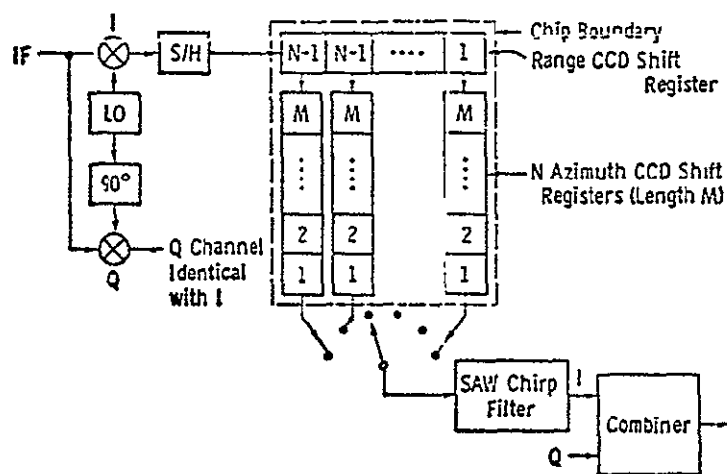
Additional research should be conducted to test some other approaches to sidelobe reduction for this system

Example of Electronic Fresnel-Zone-Plate Processor (SCANSAR)

Spacecraft Altitude:	435 km
Carrier Wavelength:	6.3 cm
Real Aperture Length:	3 m
Ground Velocity:	7.2 km/s
PRF:	7.2 KHz
Range of Nadir Angle:	7° - 22°, 22° - 37°
Swath Width:	122.3, 152.0
Number of Looks	4.2
Range Resolution:	150-63 m, 50 m
Azimuth Resolution	37.4 - 39.9 m, 39.9 - <u>46.3</u> m
Number of Scan Cells	5, 10
Fresnel Zones Processed	4
Power Consumption (both sides):	~ 131 Watts

1.1.6.5 CCD-SAW PROCESSOR PROPOSED AT RRE

- A processor for range-Doppler radar has been proposed and preliminary tests made at Royal Radar Establishment in England: this processor appears a likely candidate for SAR
- The CCD-SAW processor has been examined but not studied in detail, since we became aware of it too late for extensive study
- The processor seems to offer advantages both in simplicity and in low power consumption
- Corner turning is accomplished in a CCD analog device with many memory elements on one chip (1000 on the test version)
- Matched filtering to separate azimuth elements is accomplished in a surface acoustic wave chirp line (dispersive delay filter)
- Basic structure of the processor is illustrated below: (zero-offset version)



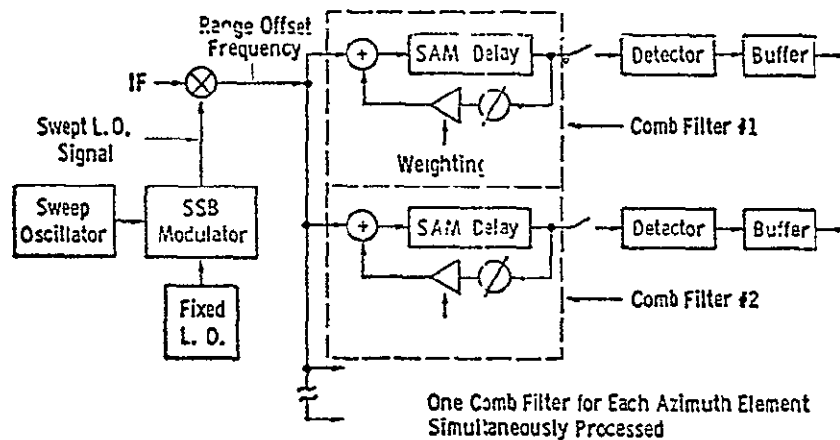
- Range shift register fills with signals from one pulse, after which these are transferred in parallel to azimuth shift registers
- Azimuth shift registers fill slowly, but are emptied quickly so a SAW frequency-sensitive delay element can "dechirp" them at same rates as when it is used for range dechirping
- Range-offset processor would not require I and Q channels but would require higher sampling rate and more range-shift-register positions.

1.1.6.6 RANGE-SEQUENTIAL SEMIFOCUSSED COMB-FILTER PROCESSOR

- A range-sequential comb-filter processor offers significant advantages because no corner-turning memory is needed
- In the comb-filter processor azimuth filtering is accomplished on each line of the spectrum of the received pulse train simultaneously in one device
- The principle of the comb filter is illustrated in the accompanying figure
- The basic form of the comb filter is shown in Figure 3. A pulse is read into a delay element such that the delayed pulse arrives at the input summing point in phase with the incoming signal; thus signals at the right frequencies add in phase after many cycles and signals at other frequencies drift in and out of phase
- The resultant filter response is shown in Figure 1 for zero phase shift ϕ . If K is constant with loop gain unity, each "tooth" of the "comb" has a $\sin x/x$ response. Tooth spacing is the PRF and tooth width is inversely proportional to the number of pulses recirculated
- The passband characteristic shown in Figure 1 is identical with that for the unfocussed processor (range sequential version) shown earlier. That is, the range-sequential unfocussed processor is in fact a comb-filter processor
- To accomplish focussed processing efficiently, Doppler shifted filter bands are required, as shown in Figure 2. The Doppler offset for the filter is set by the value of ϕ , which must be the same for all the spectral components
- Delay lines are temperature sensitive, so the best way to implement the delay for the comb filter is with shift registers (analog or digital). In the detailed SCANSAR design, SAM analog shift registers are used

RANGE-SEQUENTIAL SEMIFOCUSED COMB-FILTER PROCESSOR (CONTINUED)

- A comb-filter processor could also be built using SPS (serial-parallel-serial) CCD shift registers and gamma correctors as described later for the Texas Instruments - JPL processor. The number of SPS elements required would be much less for the comb-filter processor
- The problem of implementing the frequency-independent phase shift has been solved, but in a rather complex way. Research is needed to establish a simpler way to accomplish this phase shift
- The SCANSAR-proposed processor uses range offset (the signal is processed about a carrier frequency somewhat more than half the IF bandwidth). It does not require I and Q channels
- The basic SCANSAR processor is diagrammed below:



- The scanned (swept) local oscillator removes the azimuth chirp from the incoming signals
- SAM devices contain their own sample-and-hold circuits. These are clocked at about twice the IF bandwidth
- Buffers also use SAM devices

RANGE-SEQUENTIAL SEMIFOCUSED COMB-FILTER PROCESSOR (CONTINUED)

EXAMPLE (SCANSAR)

Spacecraft Altitude:	435 km
Frequency:	4.75 GHz
Incidence Angle Ranges:	6.7° - 22.4° 22.1° - 37.0°
Swath Widths:	129 km 157 km
Processor Power (both sides):	184 W
Range Resolution:	150 m @ 7° to 49 m @ 22°
Azimuth Resolution:	50 m @ 7° to 53.5 m @ 22°
Number of Looks:	6
Equivalent 1-Look Pixel:	150 x 6.9 m to 49 x 7.4 m

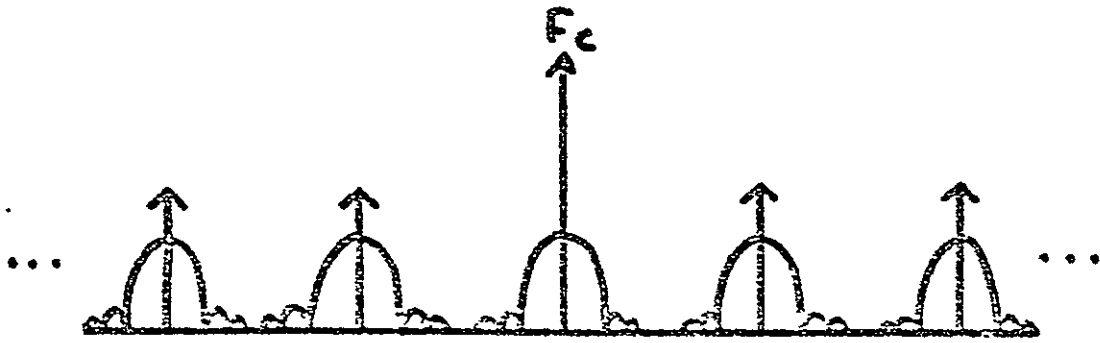


Figure 1. Comb filter passbands showing carrier and its side-bands (zero phase shift).

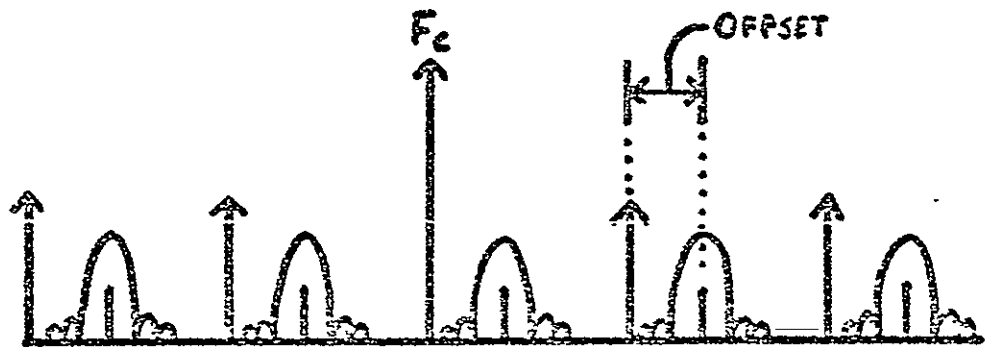


Figure 2. Comb filter passbands phase-shifted to account for Doppler shifting.

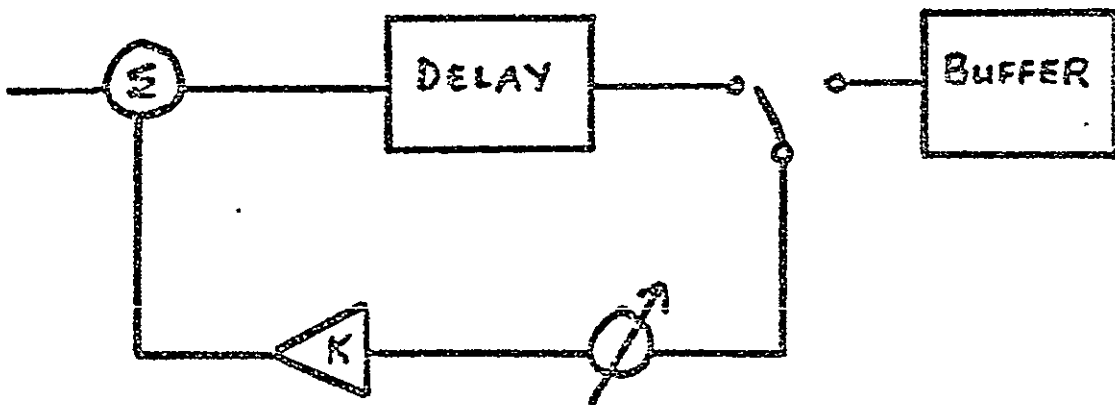
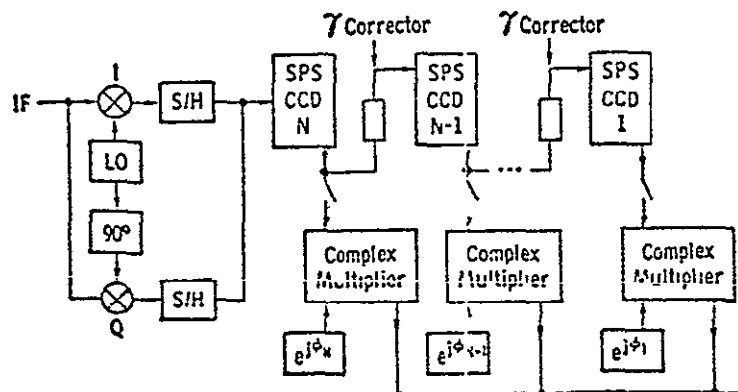


Figure 3. A comb filter delay line.

1.1.6.7 CCD RANGE-SEQUENTIAL SYNTHETIC APERTURE PROCESSOR (TI/JPL)

- This processor was developed in preliminary conceptual form under AAFE and JPL programs
- Operation of the processor is more like a synthetic antenna array, rather than a Doppler beam sharpener or matched filter, than other focussed processors
- Power consumption for the prototype system was estimated as only 7 watts for a 10 km swath with 25 meter resolution
- Low power consumption was achieved by use of large-scale integrated analog circuits designed for low power consumption; presumably several of the other implementations studied could reduce power consumption significantly by use of special LSI chips
- Major problem with CCD devices is the amount of charge left behind during the charge transfer process. This processor solves this problem 2 ways: use of SPS (serial-parallel-serial) CCD registers and use of a "gamma-correction" circuit to compensate after passage through each CCE register
- Details of this processor became available to us too late for extensive study
- Operation of the processor is presented below in simplified form:



ORIGINAL PAGE IS
OF POOR QUALITY

- Implementation shown for aperture N pulses long
- Each SPS CCE register contains samples for one entire range line; I and Q samples are alternated in the register
- After N pulses have been received and stored, outputs for each range line transfer in parallel through the complex multipliers that correct the phase for the position in the aperture and the outputs added in parallel
- Outputs are read out one range element at a time, so that each output sequence is a synthetically processed range line
- In most applications the processor must be replicated for multiple looks
- Use of SPS CCD elements with gamma correction might permit improvements in some of the other processors discussed here, but this has not yet been studied
- Use of interleaved I and Q samples with complex multiplications might permit improvements in some of the other processors discussed here, especially the comb-filter processors, but this has not been studied

A POSSIBLE X-BAND SCANSAR FOR POLAR MISSIONS

•	Frequency	9.1GHz
•	Coverage	40-55°
•	Azimuth Resolution	50-67m
•	Range Resolution	50-39m
•	Independent Looks	1
•	Equivalent Square Photographic Pixel*	233-239m
•	Spacecraft Altitude	435km
•	Swath Width*	275km (plane earth) 299km (spherical earth)
•	Antenna Size	6m long by 1.8m high
•	Beam Positions	15
•	Transmitter Average Power	18 watts (without cross-polarized sensitivity) 180 watts (with cross-polarized sensitivity)
•	Bus-bar Power	182 watts (without x-pol.) 830 watts (with x-pol.)
•	Telemetry Rate	7.0 Mb/s

All calculations based on plane-earth geometry. Minor modifications for spherical-earth geometry do not affect conclusions.

*Note: Narrower swath would permit smaller equivalent photographic pixel, but this system gives coverage at 3-day intervals at 50° latitude with idealized orbit.

1.2 BASIC CONCLUSIONS

- 1) The state of the art of knowledge of radar backscatter from sea ice and icebergs is adequate to permit immediate development of spacecraft radars to monitor them.
- 2) The state of the art of synthetic-aperture radar and its components will permit immediate development of radars for small spacecraft for the polar missions.
- 3) The best frequency for a polar mission is unknown, but almost certainly it exceeds 4 GHz and it may well exceed 9 GHz.
- 4) The best angles of incidence for the polar mission certainly exceed 22° and probably exceed 30° .
- 5) The best angles of incidence for glacier studies probably depend on the surrounding terrain relief.
- 6) The resolution for the different elements of the polar mission is unknown. Poor resolution has been used successfully for monitoring Great Lakes ice (75 m x up to 300 m).
- 7) The resolution chosen for a mission should be as poor as possible because system complexity increases rapidly with improving resolution.
- 8) The SCANSAR approach is viable as a way to achieve the coverage required for those elements (to be determined) of the polar missions for which resolution compromises inherent in SCANSAR can be tolerated.

- 9) The best approach for on-board processing is still an open question requiring further study, but several approaches are known to be workable.

1.2.2 RECOMMENDATIONS

- 1) The time has come to proceed with development of spacecraft SAR for the polar mission.
- 2) Since the SCANSAR concept seems to offer the best hope for achieving the required coverage, its development should be vigorously pursued.
- 3) Much research is still needed on interaction between radar signals and surface features relevant to the polar mission:
 - a) The required resolution for the different elements of the mission should be established as soon as possible.
 - b) A definitive statement of the true requirements for intervals between repeated coverage needs to be produced as soon as possible.
 - c) Research into radar return from sea ice should be pursued vigorously, and at once, particularly using radar spectrometers located on the ice, in combination with careful surface and coring measurements, to determine the optimum frequencies, polarizations, and angles of incidence.
 - d) Research into radar observation of icebergs should be instituted soon. This research should involve a combination of measurements made on the icebergs with spectrometers (along with surface measurements) and fine-resolution images made with as complete a set of frequencies and polarizations as possible with existing radar systems.
 - e) Research into radar observations of glaciers should be reinstated. This research should involve the same combination of instruments as for measurements of icebergs.
- 4) Research and development are needed on SAR systems for the

spacecraft water resources mission, although existing technology is adequate for initial flights:

- a) Further research should be conducted on swath-widening techniques. In particular, emphasis should be placed on evaluating in detail the effects of scanning and pointing on the radar system parameters, the potential of multiple-frequency systems for different parts of the swath, and the potential of multiple simultaneous beams to cover different parts of the swath with one frequency.
- b) Antenna optimization studies should be conducted for multi-beam and scanning systems. Relative merits of reflectors with multiple feeds and multiple-beam arrays (scanned or switched) should be evaluated.
- c) Erection techniques for the different kinds of antennas should be evaluated and compared.
- d) Experiments should be conducted to evaluate the merits of different schemes for calibration of synthetic-aperture radars.
- e) The SCANSAR should continue to be evaluated and a complete preliminary design made. Critical areas should be evaluated experimentally.
- f) Traveling-wave tube development should be undertaken to make available a family of space-qualified tubes at frequencies and power levels appropriate to the water resources mission.
- g) Analytical and experimental development should proceed on various forms of "distributed radar" (separate transmitting and/or receiving elements for different parts of the antenna), as this approach both provides redundancy and the possibility for earlier use of solid-state transmitter amplifiers.

- h) Details of the motion compensation problem should be analyzed for specific candidate spacecraft, including both the requirements of the radar and the availability of adequate compensation signals from the spacecraft orientation and other systems. If inadequate compensation signals are available, study of means for obtaining them either from the spacecraft or internally to the radar should proceed.
- 5) Research and development are needed on SAR processing systems for use on-board the water-resources-mission spacecraft:
- a) The comparative studies undertaken here should be continued and expanded. Particular attention should be given to determining power requirements for the different systems under identical mission conditions.
 - b) Potential application of single-sideband methods to SAR should be studied in more detail analytically, and experiments should be conducted in the laboratory to verify performance estimates.
 - c) The use of binary phase codes for large time-bandwidth-product radar pulse compression should be studied in detail, since this approach is more natural than chirp frequency modulation for some of the processing elements.
 - d) Application of the CCD shift registers, particularly those using the SPS technique and gamma correction, should be studied for all types of processor considered here, since they seem to offer advantages in power consumption.
 - e) Methods for implementing the comb-filter processor should be studied in the laboratory, and new techniques for accomplishing the all-pass phase shift required should be sought.
 - f) A more detailed study of the multi-look unfocussed processor should be conducted, and laboratory models constructed and tested.

- g) The correlation processor should be re-examined for possible design improvements. The impact of using CCD devices in this processor, particularly for the corner-turning memory should be investigated.
- h) The CCD-SAW processor of RRE should be studied in detail and adapted for SAR use on spacecraft. Laboratory tests are in order soon.
- i) The FFT processor should be re-examined, particularly with regard to use of CCDs for the corner-turning memory, and possibly for full analog implementation.
- j) The TI-JPL CCD range-sequential processor development should be continued, and emphasis should be placed on systems suitable for the water resources mission.
- k) The application of SAW devices to various processor configurations should be investigated as a possible way to reduce complexity.

2. RADAR CAPABILITIES FOR THE POLAR MISSION

2.1 Radar Mapping of Sea Ice - State of the Art

The use of imaging radar for observing the characteristics of sea ice has been established by numerous experiments involving radars from the U.S., the U.S.S.R., Canada, and the Netherlands. These experiments, and the operational application in the Soviet Union depend on interpretation of images to distinguish between ice of different types, and therefore of different thicknesses. Although several experimenters have reported use of low-altitude vertical-incidence sounders to determine the thickness of lake and sea ice directly, only one quantitative study has been conducted of the relationship between backscatter strength and sea-ice type and thickness; and this experiment depended on aerial photography to identify the ice types and permit inference of the thickness. Nevertheless, the extensive body of knowledge accumulated using imaging radars is adequate to justify proceeding immediately to development of spaceborne imaging radars for sea-ice monitoring.

The two parameters of interest in the study of ice cover of the Arctic ocean are the variations of ice thickness and the roughness or topographic relief of the ice cover. The distribution of ice thickness in the Arctic ocean is needed to correctly model the mechanics of ice interaction so that the drift and the dynamics of Arctic ice pack can be predicted (1). Measures and variations of ice thickness are also needed to accurately calculate the mass budgets of the ice packs as an input to climatic models (2). In addition, accurate information on variations in ice thickness is required for a wide variety of applications and operations such as those involving ice-breaking by ships and the transport of heavy equipment over ice. This information will help in economical route selection and safe load predictions.

The knowledge of the surface roughness characteristics is important for determining the momentum the wind imparts to the ice cover. This momentum is usually the most important driving force in the ice drift. Recently a program is underway to develop a large air cushion

vehicle to traverse the Arctic pack. In the design of such a system the knowledge of the surface roughness is necessary (3).

Sea ice covers a large area. Thus, the usual sure method of determining sea ice thickness and roughness by direct measurement is extremely time-consuming, expensive and has several other limitations. A need also exists to know these parameters on a continuous and regular basis. This can only be provided by means of remote measurement techniques.

The two major forms of ice in the Arctic and Antarctic oceanic regions are sea ice and glacier ice. Sea ice is formed on the ocean itself by freezing of the saline water of the sea. Glacier ice is formed on the land by compaction of snow and appears on the sea as icebergs and ice islands. Fresh-water ice formed in rivers is also found in some parts of the sea.

The formation of sea ice is a complex process depending on such factors as salinity on the surface and its distribution with depth, surface temperature, depth of water, wind, currents, waves, and air temperature (4).

Sea ice starts to form earlier on the surface of shallow than on deep water, so under similar conditions the ice begins to form near the coast first. Water with a density of brine greater than 24.7 percent has to be cooled to lower temperatures, from top to bottom, than the normal freezing temperature of water before the surface starts freezing. The temperature of maximum density in sea water with a salinity of less than 24.7 percent lies above the freezing temperature. The temperature of maximum density in pure water is $+3.98^{\circ}\text{C}$. Thus, when a layer of sea water with a salinity of less than 24.7 percent is subjected to cooling, the density at the surface increases resulting in free convection. As water is further subjected to cooling, this convection continues until the temperature of maximum density of the convective column is reached. The amount of brine present in water only affects the initial independent of the salinity of the water. The process of freezing can be delayed if

the winds produce ocean currents which carry the warmer water to the surface.

The first sign of freezing varies according to different conditions to which the water is subjected. A calm sea surface subjected to rapid cooling results in the formation of small, needle like crystals. According to Weeks and Assur (5), the first crystals of pure ice to form are minute spheres which rapidly change their shape to circular disks. After a disk has grown to a critical diameter - which is dependent on the salinity - form of the disk becomes unstable and it changes to a dendritic hexagonal star (5). The critical diameter for these disks is on the order of 2 to 3 mm for fresh water but decreases with increasing salinity. These crystals grow rapidly and close together to form a more or less uniform sheet of ice, known as young ice.

On the other hand, when waves or strong currents disturb the sea surface, the first sign of freezing is an oily, opaque appearance of water. This is known as grease ice. Upon further freezing, grease ice develops into nilas or ice rind. This development again depends on wind exposure, waves and salinity. Nilas appears as an elastic crust with a matte surface; whereas ice rind has a brittle, shiny crust.

At this stage, except in wind-sheltered areas, the thickening ice usually separates into masses as a result of the irregular motion of the surface water. The freezing occurs in separate centers from which it spreads outwards, forming circular flat disks with raised edges. These disks are 1 to 3 inches in diameter and this type of ice is called pancake ice. When freezing continues because of continued low temperatures, the cake pieces freeze together, after repeated breaking from continued motion and from chafing and collisions, to form a continuous sheet. This sheet of ice is normally less than one foot thick. The thickness of ice may grow to four or five inches within 48 hours, after which the growth is slower.

Under the influence of wind, currents, waves and pressure the sea ice may break up and drift from its original location to disperse

in some regions and crowd in others. Because of this shifting of ice, pressure may cause the ice to pile up as ridges and hummocks. Another effect of pressure, the overriding of one piece onto another, is known as rafting. Rafting causes the ice thickness to become double that of the original piece. According to Weeks and Assur (5), the main body of an ice sheet grows in a columnar form with vertical ice crystals. The orientation of the crystallographic c-axis of the ice crystal is perpendicular to the growth axis but otherwise random. During the growth of the sea ice, the impurities in the form of brine are partially rejected to the water underneath. That is why the salinity of sea ice is always less than the salinity of the original sea water from which it was formed. The distribution of impurities such as brine pockets and air bubbles has some effect on electrical and mechanical properties of sea ice.

Sea ice seldom becomes more than two meters thick during the first winter, but may assume far greater vertical dimensions because of piling-up of broken ice in the form of hummocks (6). In the spring and summer, snow cover and sea ice start melting. This continuing thawing produces passages and holes in which the surface water drains. In the next winter, this ice again starts freezing, growing to a thickness of more than two meters. It may attain greater thickness through ridges and hummocks. Thus, first year ice (ice of one winter's growth) is always less thick than multi-year ice (ice of more than one winter's growth which has gone through at least one summer's melt). First year sea ice is more salty than multi-year sea ice. First year sea ice, which is less than one year old, melts more readily than old ice.

Sea ice contains "pockets" of brine in its matrix, since the brine is concentrated in the freezing process, and the more concentrated brine solution freezes at a lower temperature than either fresh water or water with normal oceanic salt content. The bottom of the sea-ice mass normally contains a high concentration of brine, since it is in contact with or close to the sea water. Furthermore, the brine pockets migrate

from within the ice mass to the bottom. Some of the thinner forms of sea ice also contain higher concentrations of brine near the top because salt spray can be carried onto the top and freeze there. On the other hand, the older ice is usually in large thick layers not subject to this surface coating with recently frozen sea water. This is illustrated in Figures 1 and 2 from Weeks and Assur (5).

The ice mass can be quite complex because of the effects of mechanical stresses and breaking of the ice sheets. Often a sheet of ice breaks and one portion is driven on top of another (rafting), so the profiles of salinity and temperature are composites of the two original profiles. Eventually, if this ice lasts through more than one year, these inhomogeneities are reduced by natural diffusion processes (see Figures 3 and 4). Another significant mechanical effect is the formation of pressure ridges. These ridges not only extend to considerable heights above the main ice surface, but also extend even farther beneath the bottom of the pack ice.

Thick first year ice is generally rougher than the multi-year ice. The major difference is due to the fact that the multi-year ice has undergone at least one cycle of erosion whereas the first year ice has not. The deterioration effects on the sea ice surface caused by the ice having gone through a summer's melt (6) are the following:

- a) the weathering, rounding and subdividing of normally sharp, high-standing pressure ridges;
- b) the ablation of small pressure ridges through weathering, creating isolated hummocks on the ice;
- c) the creation of fresh water puddles or melt pools and their subsequent refreezing and
- d) the presence of a subdued drainage pattern on the ice surface.

There is a lack of general quantitative information available on the surface roughness parameters of sea ice. No such information is available on the microwavelength scales. This information is needed to compute radar return from sea ice utilizing theoretical scattering models. A very general idea of the roughness parameters and the spatial

variations in roughness (such as size, number and frequency of ridges) can be obtained from (3), (7), and (8).

Electrical properties of sea ice have been measured by many workers at frequencies below those of interest in the spacecraft radar situation, but only in 1971 did Hoekstra and Cappillino (9) measure the complex dielectric constant of sea ice over the 100 MHz - 23 GHz frequency range. The electrical properties of sea ice as reported in the literature have one feature in common: the complex dielectric constant of sea ice is dependent on both temperature and brine concentration. Brine concentration itself depends on temperature, and on the salinity of the sea water forming the ice. Since brine concentration and temperature vary with depth and with ice thickness, the electrical properties also vary with depth and thickness. Results of Hoekstra and Cappillino's measurements are reported here (9).

In Figure 5a the dielectric loss of sea ice samples as a function of temperature for different salinity is given at a frequency of 400 MHz. The dielectric loss at a frequency of 9.8 GHz is given in Figure 5b. The dielectric loss and dielectric constant at a frequency of 2.3×10^{10} Hz are given in Figure 5c. As is evident from these figures the dielectric loss of sea ice increases with an increase in salinity and temperature. The dielectric loss is more at 400 MHz than at 9.8 GHz. The dielectric constant increases with an increase in the temperature. As a result electromagnetic waves at the same wavelength are liable to penetrate the first year ice less than multi-year ice. Also, in the winter the relative penetration of waves is going to be more than in summer because of lower temperatures and thus lower loss tangent.

The complex dielectric constant in general determines the strength of the scattered or reflected signal and the penetration or attenuation of the electromagnetic wave inside the medium. An attempt was also made by Hoekstra and Cappillino (9) to compute theoretically the dielectric properties of sea ice and the results reported are shown to be in general agreement with the experimental results in certain frequency ranges.

The dielectric constant of brine varies from 80 at 10^8 Hz to approximately 34 at 2.3×10^{10} Hz. The dielectric constant of pure ice in this frequency range remains at about 3.5. Thus, the dielectric constant of inclusions (brine) is several times larger than the dielectric constant of the continuum (ice). The dielectric constant of the mixture thus depends on the amount and the shape of the inclusions.

SLAR was developed in the early 1950's primarily for military use. It was first used to map sea ice in the early 1960's when the U. S. Army Cold Regions Research and Engineering Laboratory (CRREL) conducted experiments over the Arctic pack ice utilizing the existing AN/APQ-56 radar system. The capability of a radar imager to map large areas of sea ice in short periods of time was shown then. It was shown by Anderson (10) through the analysis of the obtained images that major sea ice types can indeed be identified on the radar imagery. He showed that the sea ice imagery is interpretable to the extent that winter ice (only one season old) can be differentiated from the thicker, older, polar ice. The concentration and distribution of sea ice can also be determined. The rough-surfaced polar ice, generally from 2.5 to 4 meters thick, with pressured ice areas being much thicker, gave a light tone on the images. The relatively dark-toned areas consisted of relatively smooth refrozen leads and polynyas with younger, thinner ice. Open water gives still darker tones. This experiment was conducted in winter. No quantitative analysis which would help in the design of future radar systems was done by him. The AN/APQ-56 radar system used in collecting the data is a real-aperture system operating at 8.6 mm wavelength.

It is pointed out by Bradie (11) that one hindrance to interpretation of ice features on radar is the great tonal variance between open water, young ice, grease ice and slush ice.

During September 1969, the U.S. Coast Guard, in conjunction with the Manhattan tanker test, conducted ice-mapping experiments in the Northwest Passage using a modified Philco-Ford AN/DPD-2 SLAR, operating in the Ku-band (16.5 GHz frequency). In addition to the research effort

to determine its feasibility as an ice observational technique, the SLAR was also used as a routine aid to the Manhattan. This experiment was conducted to assess the performance of SLAR in mapping and identifying sea ice. As shown by Johnson and Farmer (12), the results of this experiment indicated that SLAR can readily be used to detect ice concentration, floe size and number, and water openings.

It is also possible to identify, through careful image interpretation, ice age, ice drift, surface topography, fractures, and pressure characteristics. Young ice gives even dark tone and may have bright straight lines indicating ridging. Dark-gray to black and smooth tone is given by first year ice and ridging indicated by light straight lines. Second year ice gives even graytone and may have ridging. Ridges are more jagged than in first year ice and also higher than first year ice. An even tone is given by relatively smooth topography. Multi-year ice gives mottled tones of gray probably caused by high weathered ridges and interconnecting melt holes. Old multi-year drainage channels can also be traced sometimes. Dark areas of no radar return signify presence of open water. The parameter which can be most easily determined on the radar imagery is ice concentration along with the size of floe. The most difficult characteristic of the ice to determine from SLAR imagery, other than its actual thickness, is probably its categorical age. Another important feature that can be interpreted is whether or not ice is or has been under pressure. It is also possible to identify topographic features such as pressure ridges, hummocks, and cracks.

It is pointed out by Johnson and Farmer (12) that the all-weather, day-night operational capability and the broad areal coverage provided by SLAR make it an effective means of observing sea ice characteristics and for many purposes it provided observations superior to information obtained by a visual ice observer. The same experimental data was used to determine the drift of sea ice. The results were presented by Johnson and Farmer in another paper (13) and reveal that single ice floes, as well as general ice masses, could be tracked to an accuracy of nearly one

nautical mile. In the study conducted at Biaché by Bradie (14) of the SLAR imagery obtained in the Manhattan experiment, it is pointed out that major ice types, cracks and leads can be identified.

Ketchum and Tooma (15) presented the results obtained from the radar experiment conducted by the U.S. Naval Oceanographic Office during April, 1968. This experiment was conducted over the sea-ice fields north of Alaska; the four-frequency radar system of the Naval Research Laboratory was used. The results presented (15) indicate that the shorter-wavelength X-band radar appears to have the greatest potential for sea ice study when more definitive information such as mapping, distributions of stages of ice development, and fracture pattern analysis is required. The X-band radar imagery can be used to discriminate old (second year ice) from the young ice, the old ice giving higher return or backscatter. Young ice (first year ice and younger) is smooth and could not be discriminated from open water in this experiment. Pressure-ridge patterns could sometimes be identified when they were present on a low-backscatter background. There were no notable differences between horizontally and vertically polarized X-band imagery. The potential value of L-band radar is not for mapping the aerial distribution for surface topography. Various ice types do not give discriminatory graytone at this wavelength, whereas the more topographic features such as ridges and hummocks can be discriminated. Only the most prominent features, such as large floes and fractures, could be identified on the P-band (400 MHz) radar imagery. It was pointed out that for motion studies in which reidentification of specific features is necessary, the X-band or preferably K-band radars, would be the best choice. This was the only known multi-frequency study of radar images of sea ice.

In studies conducted by Raytheon company (16,17) and Photographic Interpretation Corporation (18), it was shown that SLAR is a useful tool to map changing nature of sea ice. Data acquired by the U.S. Coast Guard of the Baffin Bay and Beaufort Sea areas in February and March of 1971 were analyzed by Raytheon Company (17). Major ice types such as

new ice, young ice, first-year ice and multi-year ice could be identified on the imagery. It was not possible to make a finer delineation of the categories. SLAR imagery did permit the determination of surface configuration and it was much easier to delineate edge of the floe on the SLAR imagery than the photo. The effects of snow cover on sea ice could not be determined. Sea ice images did not exhibit any masking because of snow cover except for the return from ridges. The identification of the ice age could be accomplished, whether covered by thick or thin ice cover.

The same data were also analyzed by Photographic Interpretation Corporation (16). In their report an attempt was made to determine winter sea-ice parameters and to compare winter sea-ice pattern "keys" with the summer pattern "keys". It was pointed out that interpreters must not rely entirely on radar keys for their work but should properly assess all of the imagery parameters such as tones, textures, spatial relationships, imagery limitations, ice environment and season, and ice stress patterns. By doing this a very detailed description of sea ice can result and the predictions about the ice can be made with more reliability. Multi-year ice can be separated from other ice types more rapidly on the radar image than through use of aerial photos and stress zones can also be quickly delineated. Snow cover does not present any detrimental masking effect of sea ice conditions on the Ku-band radar imagery.

Glushkov and Komarov (19) and Loshchilov (20) demonstrated the use of SLAR imagery (wavelength = 20 mm) obtained from the TOROS* in determining the ice conditions and ice drift. The use of optical techniques to analyze the sea ice imagery was reported by Zagorodnikov and Loshchilov (21).

The TOROS experiments were started in 1968 and have been carried out extensively since that time. Moore (22) was shown ice images from

*The TOROS was developed for ice reconnaissance use. The word "toros" is Russian for "ice ridge".

various seasons and multi-year coverage of ice islands during a visit to the Arctic and Antarctic Institute in Leningrad in June, 1973. At that time he was shown an ice coverage map of the north coast of the USSR prepared in May, 1973, for the use of shipping. He was led to believe that the TOROS was by that time coming into operational use for mapping ice to permit optimal ship routing for convoys along the USSR's northern sea route.

To evaluate the capabilities of a SLAR system as an ice reconnaissance tool, a SLAR test project was organized and carried out in April, 1972 by the Canadian Department of National Defence and the Atmospheric Environment Service of Canada. The SLAR system used for the experiment was a Motorola AN/APS94D unit operating at a wavelength of 3.2 cm. The results of the experiment are presented in a report by the Canadian Department of Atmospheric Environment (23). The results indicate that it is generally possible to identify open water by low radar returns and uneven boundaries with surrounding ice that show good contrast in tone. It is difficult to distinguish new ice from open water because the surface is generally smooth and the profile of any rafting present is low. Variation in returns from large floes is apparent in the larger scale imagery. It is possible to determine floe size and concentration and to distinguish first year ice, fast ice and multi-year ice. Floes showing good radar returns can be classed as rough first year ice. Note that the AN/APS-94D has a resolution along-track of 7.5m/km and a swath to one side of 40 km. Thus, the resolution is crude at the far range, and the incidence angle is quite near grazing over much of the swath.

It is evident from the material presented above that a radar system is capable of remotely sensing sea ice. Despite this knowledge there is a lack of fundamental research in this area. No systematic studies for relating radar returns or backscatter to sea ice were undertaken until 1967. A joint mission over sea ice in the Arctic was conducted in May, 1967 by National Aeronautics and Space Administration (NASA), Navy Oceanographic Office, U.S. Army Cold Regions Research and Engineering

Laboratory (CRREL), the Arctic Institute of North America, and the University of Kansas with the objective of verifying the ability of a 2.25 cm wavelength radar scatterometer to identify sea ice types. The reason for not using radar imagers was that a more quantitative study of radar backscatter could be undertaken from scatterometer data since scatterometers permit more detailed observation of radar scattering behaviour than imagers. The radar scatterometer used is an instrument designed to measure the radar backscattering coefficient σ° (radar cross-section normalized to the illuminated area) as a function of the illuminated incidence angle θ (angle measured from the vertical) and by design it is a calibrated system (24). The radar return power and thereby the graytone on the radar image, is directly proportional to σ° . σ° is an important parameter in the design of a radar system and it depends on frequency, polarization, angle, and electrical and physical properties of the target such as complex electric permittivity, surface roughness and subsurface structure. All of the SLAR's in operation today are uncalibrated systems. As a result it is not possible to compare images obtained from two different systems or to compare images produced by the same system at different times. Moreover, it is impossible to obtain quantitative information which would help in the design of future systems. Because radar scatterometers are calibrated systems, the data obtained from them is of great value in understanding the nature of radar return from different targets and in the design of future systems.

An analysis of the scatterometer data obtained from the May, 1967 mission was carried out by Rouse (25). It was shown that a 2.25 cm wavelength scatterometer can be used to discriminate ice types. It was seen that multi-year ice gives higher return at all angles than the first year ice. Open water can be distinguished easily. This experiment was limited to a single frequency (13.3 GHz) and vertical polarization.

In April 1970, another experiment was conducted jointly by NASA, Naval Oceanographic Office, and the University of Kansas. This experiment was designated Mission 126 and was carried out in the vicinity of

Pt. Barrow, Alaska. Large amounts of data were gathered by this mission so that a systematic study of radar return from sea ice could be undertaken. This study was conducted by Parashar (26). The ability of radar to discriminate sea ice types and their thickness was presented. Radar backscatter measurements at 400 MHz (HH, VV, VH and HV polarizations) and 13.3 GHz (VV polarization) were analyzed in detail. The scatterometer data were separated into seven categories of sea ice according to age and thickness as interpreted from low-altitude stereo aerial photographs. There is a reversal of character of radar return from sea ice less than 18 cm thick at the two frequencies. Multi-year ice (sea ice greater than 180 cm thick) gives strongest return at 13.3 GHz. First-year ice (30 to 90 cm thick) and open water give strongest return at 400 MHz. Open water can be differentiated at both the frequencies. Although 400 MHz is not found to be as satisfactory for ice identification as 13.3 GHz, combining a 13.3 GHz and a 400 MHz system definitely eliminates the ambiguity regarding very thin ice.

Four-polarization 16.5 GHz radar imagery was also analyzed. The results (26) show that open water and three categories of sea ice can be identified on the images. The results of the imagery analysis are consistent with the radar scatterometer results. There is some indication that cross-polarization return may be better in discriminating sea ice types and thus thickness, but the quality of the images was not sufficient to guarantee the validity of this conclusion.

An attempt was also made to formulate a theory for polarized radar backscatter cross-section σ° for sea ice by taking into account the amount of brine entrapped, temperature, and surface roughness. The computed results from the theory are shown to be in general agreement with the experimental results.

Automatic classification techniques were applied to scatterometry data. Using the four categories (as in the SLAR analysis) 85 percent agreement can be achieved between the radar and stereo-photo interpretations.

Since these experiments, numerous other imaging radar flights have been made over the Arctic using the AN/APS-94C real-aperture 3-cm-wavelength SLAR. Even with the relatively poor resolution of this system (7.5 milliradians along-track, 75-meter slant-range across track), much useful information has been obtained, but no addition has been made to the quantitative data base. Results with this system should also be viewed with caution regarding their application to spacecraft radar systems, since the combination of relatively low aircraft altitude and long ranges means that the majority of each image is at angles of incidence well beyond 70° , and these angles are difficult to attain with a spacecraft system because the long ranges require excessive amounts of power.

During the 1975-76 winter the Canada Centre for Remote Sensing made flights over the ice with a 13.3 GHz multipolarized scatterometer. Details of these measurements have not been reported, but de Villiers states (27) that the cross-polarized results bear out the observation initially reported by Parashar (26) with the DPD-2 imaging system that the ambiguity between very-thin-ice signal strength and that for about 1 meter thickness in the vertically polarized observations does not exist for cross-polarized signals; i.e., the cross-polarized return increases monotonically with thickness from the very thinnest ice on up to the multiyear ice.

The state of the art of imaging sea ice can be summarized as follows:

1. Radar can be used to measure the following parameters of sea ice:
 - a. Concentration: It is most easily determined.
 - b. Floe Size: It can be readily observed.
 - c. Water openings: They are quite easily determined as black areas of no radar return.
 - d. Drift: It can be determined by the repeated radar coverage of the same area and by identifying similar features. Single ice floes, as well as general ice masses, can be tracked to an accuracy determined by repetition period, resolution, and navigational accuracy.

e. Topographic features: The ability to detect individual pressure ridges is limited by the sensor resolution. Pressure ridges are noted by their white or light gray linear images. Hummocks can be detected on good SLAR imagery.

f. Fractures: Fractures are quite often imaged as alternate dark and light returns, depending on their width and orientation to the radar beam. Careful scrutiny of the imagery is necessary when interpreting this feature.

g. Pressure: SLAR imagery can be used to interpret whether or not ice is or has been under pressure.

h. Ice age: It is probably the most difficult characteristic that can be determined from SLAR imagery. The resolution of the SLARs used previously generally restricts their ability to discriminate between individual minute surface features, such as puddles and drainage channels, that are characteristic of certain stages of development. However it is possible to determine categorical age by identifying certain other features such as size, shape, and texture of the imaged ice; its location as compared to the surrounding ice; place where imagery was taken and time of the year. It is also possible to discriminate and identify different ice types from the relative gray tones of the image. Normally at X-band and higher frequencies, multi-year ice gives the strongest return. New ice which is rough, sometimes gives as bright a return as given by multi-year ice, but it can be discriminated from multi-year ice because it does not have any sharp edges. More research is needed before a general set of guidelines can be developed for interpreting ice age or category age from the radar imagery. The effects of frequency, polarization, angle, resolution and seasonal variation have still to be fully understood.

i. Ice thickness: It is not possible to get a direct measure of the ice thickness from a radar image. It is possible, though, to get a rough measure of the ice thickness by associating a mean thickness with an ice category with brightness on a radar image or value of σ^0 on scatterometer data. This can only provide a rough estimate but still is useful information. It is also possible to obtain an empirical relationship between the brightness on a radar image, or between σ^0 on scatterometer data and ice thickness.

2. Frequency: Higher frequencies appear superior to lower frequencies both in terms of ability to discriminate ice types and because the signal returns are much greater, thereby permitting lower-power radars. Frequencies in the 9-17 GHz region have been used successfully to discrim-

inate ice type, and the limited 400 MHz data available indicate ambiguities at that frequency that would be difficult to resolve. If cross-polarized imagery were not available, combining 400 MHz with a higher frequency would permit resolving the ambiguity between very-thin ice and 1-meter-thick ice, but this could also be done by interpreting image texture. The optimum frequency or combination has not been determined.

3. Polarization: The two like polarizations (VV and HH) appear about equal in their discrimination capability. Cross-polarized signals appear to be able to overcome the mentioned ambiguity, but require more power (how much remains to be determined).

4. Resolution: No quantitative study has been undertaken to determine required resolution. Modest-resolution systems have been successful, but the improvement possible with better resolution has yet to be established.

5. Snow Cover: The masking effect of snow cover remains to be determined. Any of the frequencies considered should be able to penetrate cold, dry snow, but the effect of snow cover during the summer melt period is unknown.

6. Seasonal Variation: The changes in the appearance of ice on radar with seasonal variation needs to be determined. Preliminary indication is that the same guidelines can be used for discriminating ice type in winter and late spring. Russian experience with this is most extensive, but has not been reported.

7. Automatic Classification of Ice: It has been shown that automatic classification techniques can be used in discriminating sea ice types in analyzing scatterometer data. An agreement of about 85 percent has been achieved in identifying and classifying four categories of sea ice as established from stereo-photo interpretation. Such automatic classification schemes have yet to be tried on the radar images of sea ice. These classification techniques can also be used in establishing optimum discriminatory parameters such as frequency, polarization, and angles.

2.2 RADAR MAPPING OF ICEBERGS - STATE OF THE ART

Although several experiments have been conducted on the mapping of icebergs with radar, and although the ability to see icebergs on radar imagery has been established, no extensive program has been conducted aimed at establishing the proper radar system and operational parameters for locating and identifying icebergs. The earlier studies, and many of the later ones, used ship-based or land-based radars; both the radar characteristics and the low angle of incidence for these measurements make their applicability to the definition of capabilities and parameters for spacecraft imaging radars to detect and identify icebergs minimal. Various programs have been conducted with SLAR since 1957, but in each case the radar used was selected because of its availability rather than because its characteristics were in any sense expected to be optimal. Furthermore, these tests have not attempted to determine required resolution or angle of incidence for iceberg measurement even at the frequencies of the available radars. Thus, the state of knowledge about radar's capability to monitor icebergs is rather minimal, though encouraging.

Icebergs are usually "land ice" and most Northern Hemisphere bergs result from breaking off of glaciers as the glacial ice flows into the sea. In the Southern Hemisphere, many of the bergs break away from the shelf ice, so their shapes and size are quite different (flatter and bigger) than those of Northern Hemisphere bergs. Most of the interest in tracking icebergs relates to the Northern Hemisphere, for there is little shipping in areas where it may be endangered by Southern Hemisphere bergs.

Because icebergs are formed on land, their physical characteristics are those of land ice, rather than those of sea ice. Hence, they have low conductivity, and at low temperatures radar signals can penetrate much further into them than into sea ice. Furthermore the scattering coefficient of the icebergs is much less than that of sea ice because of

the lower reflection coefficient of the fresh-water ice. In spite of this, they apparently scatter sufficient microwave energy so that they are readily visible.

The first field experiment using radar to detect icebergs was conducted in 1945 by the Ice Information Group (Task Group 24.7) with the goal to devise a method for the quantitative analysis of shipboard radar as an iceberg detection instrument. During the 1946 season supplemental work was done by the International Ice Patrol (IIP). The National Research Council of Canada performed qualitative tests of shipboard radar for ice navigation between 1953 and 1957. These studies indicated that icebergs are not consistent targets. An in-depth experiment was conducted in 1959 by the U.S. Coast Guard, in which the microwave reflective characteristics of glacial ice were determined by using radar(1). Results of this study indicated that icebergs are poor reflectors of electromagnetic energy. All these experiments were conducted by shipboard radars but now experience has shown that aircraft radars like SLAR tend to detect icebergs more reliably than shipboard radars.

Dempster at the Memorial University of Newfoundland (2) has used an X-band radar on ships and on a cliff 730 m above sea level in Labrador to detect icebergs almost without fail, the only exceptions being a few low-profile domed bergs in heavy swell. His conclusions on the use of this type of radar are more encouraging than those reported by Super and Osmer (3), who stress problems with ship-mounted radars in the Grand Banks area. Perhaps some of the difference may be ascribed to radar characteristics, for the modern radar used by Dempster has a 10.5 m range resolution at the shorter distances.

The U.S. Coast Guard first conducted experiments with Side Looking Airborne Radar (SLAR), for use on the International Ice Patrol mission, as early as 1957. It was apparent then that the high resolution of SLAR imagery would provide a number of clues useful for the discrimination of icebergs from man-made objects like ships. These tests were conducted using the AN/APQ-55 (XA-1) K-band real-aperture radar system. Only a

limited amount of data was collected at that time and most of it was not useful because of the experimental nature of the system. The U.S. Coast Guard did not conduct any further experiments using SLAR until 1969. In 1969, an unfocussed synthetic-aperture SLAR system, AN/DPD-2, operating at Ku-band was utilized to test its capabilities as an iceberg discrimination tool for the IIP. These test flights were repeated in 1970, 1971, and 1973 (3).

Subsequently, in 1975, the AN/APS-94C used by NASA Lewis Research Center was flown experimentally in support of the International Ice Patrol in the Grand Banks and Labrador Coast area. The system was used successfully, including detection of small bergs to 48 km range, but target identification remains a problem (3). This is not surprising in view of the coarse resolution of the system (7.5 m/km in azimuth, 37.5 m in range).

The main problem in the detection of icebergs is that they sometimes give the same return as given by ships. Thus the important thing is to devise methods for interpreting radar imagery by which the icebergs can be identified and discriminated from other objects. The usual basic clues of radar imagery interpretation, such as size, shape, shadow, tone, texture, and pattern, can be used to identify icebergs. There are also some clues which apply to icebergs on SLAR imagery but are not commonly used. These clues are the presence and shape of a wake and the edge sharpness of an image.

The overall size of icebergs and ships may vary considerably in each case. If the length-to-width ratio exceeds 5 to 1, the object is usually a ship. An approximate measurement of the height can be made if sufficient detail in the radar shadow is present. If the radar shadow exceeds 25 meters, then the object is usually an iceberg.

It should be pointed out that the dimensions of the object being measured must be greater than the resolution of the radar at the range to the object if these clues are to be used. The shapes of the iceberg on the radar images often tend to be repetitive. Several shapes can be identified. Medium and large icebergs generally have square or rec-

tangular shaped images. Small bergs and growlers tend to have either circular or oval shaped images. The SLAR images of the icebergs are highly irregular and complex within the confines of the above shapes. Ships and fishing boats have uniformly shaped returns on the SLAR imagery and the larger vessels frequently exhibit definitive shape.

Icebergs often exhibit a shadow or a no-return area behind them. When the iceberg is surrounded by sea ice, it almost always has a shadow, depending on the height of the iceberg and the angle of incidence. Because open water gives a black tone as compared to sea ice, the shadow effect is not as readily apparent when icebergs are in the open water. Man-made features such as ships usually give a brighter tone than the icebergs. Icebergs have texture because they are many-faceted and normally have a very irregular structure. Ships on the other hand, give a more even tone, although ship echoes can also be complicated. The edges of SLAR imagery of icebergs are normally not clearly defined.

Large moving ships generally exhibit a well-defined wake on SLAR imagery with the apex at the target. Icebergs may on occasion exhibit a wake, but there is generally no defined apex and the width is fairly constant with little or no flaring.

In the data presented by Anderson (7) icebergs give brighter return as compared to surrounding sea ice. Their small size, angular shape, and concentration of high signal return help to identify them as icebergs. Since icebergs have a lower reflection coefficient than sea ice, their relatively strong return must be related to their geometry. Most of the experiments have been at angles near grazing incidence, even with the airborne radars, so the vertical and near-vertical sides of the icebergs are at a more favorable aspect angle for radar backscatter than the sea ice (except for pressure ridges, which also give strong echoes). Perhaps their surface characteristics are more like those of sea ice because of slat spray that has blown onto them and frozen than like the internal characteristics that must be representative of land ice, but this is purely speculation. Of course, many places that icebergs

are seen have temperatures well above freezing, so the melted surface would have a high reflection coefficient more like that of water than like that of either sea or land ice.

Loschilov (20) reports observations similar to those of Anderson just quoted, based on use of the Toros (translation: "ice ridge") 16.5 GHz SLAR. He states:

"According to our observations the probability of iceberg identification on SLAR imagery is the highest when icebergs are encountered in close sea ice. The icebergs give brighter return as compared to surrounding first-year and multi-year sea ice. It is more difficult to identify icebergs on radar imagery when discriminating them from single floes and ships in open water or in very open pack ice. Especially difficult is to interpret SLAR imagery during summer intense ice melting."

Presumably these comments also apply to near-grazing incidence, since the Toros SLAR has a rather wide swath and its carrying aircraft does not fly at very high altitudes.

In view of the existing observations reported here, radar clearly seems capable of monitoring icebergs under many conditions. On the other hand, nothing is known of the optimum frequencies, polarizations, angles of incidence, or resolutions. Research into these matters is thus strongly recommended.

2.3 RADAR MAPPING OF GLACIERS - STATE OF THE ART

Numerous incidental observations have been made of SLAR imagery of glaciers, and a few more detailed studies have been conducted. As with so many other applications of SLAR, however, the systems used were those that were available, and no attempt was made to determine optimum radar parameters, or the effect that a different choice of radar parameters would have on the ability to map the glaciers.

Glaciers cover 11 per cent of the surface of the earth and contain over three-fourths of the world's fresh water. In spite of their relatively slow movement, they are dynamic systems; in some cases the movement can be as much as 100 m/day, but of course most glaciers move much more slowly. Although most common in polar regions, glaciers exist throughout the world. Since they are normally found in remote and inhospitable areas frequently covered by clouds, study on the ground and from the air in the visible range is often difficult.

SLAR permits some measurements that would be difficult in the visible range even in the absence of cloud cover. For instance, new dry snow cover that obscures visual observation of glacial boundaries and features is usually penetrated by the microwave signal. Furthermore, distinctions can often be made between old snow (firn) and new snow on the radar images. Areas of meltwater, an important index of the glacier's mass budget, give characteristic low returns on the radar imagery.

Glaciers can be classified into three types based on their morphology: (1) alpine or valley glaciers, (2) piedmont glaciers, and (3) glacial ice caps. Alpine glaciers, as the name suggests, occur in valleys in mountainous areas and the larger ones flow out through the valley systems much as rivers do, except for the time scale. When valley glaciers exit from the mountains into level lowlands, they tend to spread out into large, flat, lobes of glacial ice called piedmont glaciers. Ice caps are the largest glaciers; they include mountain

and lowland ice caps and continental ice sheets. Mountain ice caps form in the high parts of mountain ranges and plateaus, covering much of the surface and sending valley glaciers down to the lower elevations. Lowland ice caps that develop in relatively flat terrain are found only in the most Northern Arctic areas. Continental ice sheets in Greenland and Antarctica represent the major part of the glacial water storage.

Glacial ice is formed almost exclusively from snow falling over the years and accumulating. This snow undergoes extensive physical change and nourishes the glacier, while gradually being transformed into glacial ice. The snow itself may have a density as little as 0.05 g/cm^3 , but in the final stages the density increases to nearly that of pure ice, 0.9 g/cm^3 . Thus, the radar observations of glaciers must include monitoring of the various forms in the glacial development, although the initial snow of low density will usually be penetrated by the signal.

The dielectric properties of the various components of the glacier structure have been measured in the microwave region by Cumming (28) and by Evans (29). In general, the dielectric constant of the cold forms (more than 20° below freezing) varies from 1.35 or so for snow up to a bit more than 3 for solid ice, with little loss. At higher temperatures the loss increases, so that near freezing, where some liquid water may be contained in the snow cover, the loss tangent may be quite significant with resulting loss of the ability for the radar signal to penetrate.

Many of the studies of continental ice sheets using radar techniques have concentrated on measurement of the thickness by an altimeter-like probe carried on a surface vehicle or a low-flying aircraft. These systems operate in a frequency range from about 30 MHz to 150 MHz, and occasionally to 450 MHz. They are not suitable for use on spacecraft, so they are not discussed further here.

Mapping of glaciers differs depending upon the type of glacier

being considered. Valley glaciers require mapping of the borders, the firn line, the glacial front, and the extent of snow cover in a particular year, as well as the extent of summer melt ponds. Continental ice sheets, on the other hand, may be mapped in terms of their crevasses and general extent, but mapping may be particularly of interest near their borders where features similar to those for the valley glaciers become important.

Meier et al. (30) evaluated the glaciological data content of several sensors in tests carried out at South Cascade Glacier, Washington. Among the sensors evaluated was the AN/APQ-97 Ka-band side-looking airborne radar and the imagery it produced. The investigators found that morphological features associated with glaciers such as moraines, crevasses, and textural patterns show up clearly. They were also able to distinguish between snow and ice and found that gross textural differences between glaciers and land were apparent even when both had a thin covering of snow. The high relief and steep slopes in the area caused some shadowing problems, however, judicious choice of depression angles can overcome this problem (31). Because of radar's ability to distinguish glaciers from surrounding terrain and icebergs from the sea independently of weather conditions and even through a thin snow cover, the authors conclude that it is possible to inventory the world's glaciers. The authors also point out that while multispectral and color photography from satellites may provide useful glaciological information, their use would be limited by the paucity of colors and tonal contrasts in snow and the operating restrictions imposed by darkness and cloud cover.

Leighty (32) described the terrain information contained in AN/APQ-56 Ka-band radar imagery acquired over northwestern Greenland. Four general terrain types were covered by the imagery: the Greenland ice cap interior, the ice cap margin, land, and sea and ice. The ice-cap interior, lying beyond the firn line, was found to be snow-covered and monotonous, having very small-scale relief due to wind erosion and

deposition. Radar imagery acquired over the ice-cap interior was uniform and without detail except along transportation routes where compacted snow gave lower returns. In addition, these transportation routes were discernable on imagery even when they were covered by at least a foot of uncompacted snow.

On imagery acquired over the ice-cap margin, crevasses were very apparent and based upon their arrangement, Leighty was able to make structural interpretations and estimations of relative rates of ice movement in various parts of the glacier. Moraines, snow drifts, and standing water were also observable, and Leighty was able to differentiate different types of glacial ice based on image tone. Leighty found the ice-cap - land contact difficult to determine where no great change in slope existed or where the area was covered by snow. Elsewhere, margin identification was relatively easy. Leighty rates the relative signal return from terrain materials in the following decreasing order: snow, glacial ice, soils and rocks, lake ice and sea ice, and open water. Leighty also concludes that different look directions are important for maximum information retrieval.

Page (33) reviewed the applications of various radar techniques to studies of ice and snow. His discussion of imaging radar is largely concerned with mapping and monitoring sea ice using NA/APS-940 X-band SLAR imagery acquired along the northeastern coast of Ellesmere Island. Some of this imagery however, covers a portion of the Grant Ice Cap and Page mentions the typical "milky appearance" of the glacial ice. This glacier has a fine-grained texture and brighter tones than those produced by glaciers on most of the Ka-band imagery analyzed in the other studies. Page also mentions that there is some evidence to indicate that radar is capable of detecting subsurface structures in glacier ice. He also points out that use of radar with a wavelength longer than the 3 cm of X-band results in decreased gray tones in images of ice.

In 1973, Moore (22) was shown radar images of glaciers obtained during the USSR monitoring of sea ice. These 16 GHz real-aperture images

showed the flow lines on glaciers very clearly. No attempt was made to analyze the images, and any Soviet analyses of them were not provided.

Radar imagery produced by the Jet Propulsion Laboratories' L-band ($\lambda=25$ cm) SLAR over southeastern Alaska was described by Elachi and Brown (34). This imagery covered areas in southeastern Alaska that include several large valley glaciers and part of the Malaspina piedmont glacier. The glaciers could be identified by a combination of shape and tonal contrasts. Medial moraines in the glaciers which are characterized by concentrations of erosional debris and surface roughness differences were visible on the imagery. Deformation of these medial moraines together with other patterns visible on the glaciers indicated stresses present in the ice and relative rates of movement. Numerous tonal variations within the glaciers were apparent on the imagery and were most likely caused by physical difference in the glacial ice. The authors maintain that since SLAR resolution is independent of range, similar imagery could be obtained from an orbital spacecraft.

It is worth noting that the above studies of SLAR's applicability to the study of glacial ice have been carried out in different environments, at various times of the year, and used radars with important system parameter differences. In addition, few of the investigations included the simultaneous collection of ground truth. As a result, the ice and system parameters that are important in determining the reflection of radar from glacial ice are poorly understood, and conclusions drawn from the study of glacier imagery are often sketchy and, in some cases, seemingly contradictory.

It is obvious that more work needs to be done before the full applicability of SLAR to glacial studies is understood. However, some of the results presented in the publications reviewed above are encouraging. In most of these studies, it was discovered that radar had the ability to penetrate snow to some degree. This is an important ability since it could make possible the delineation of glaciers from snow-covered terrain at all times of the year. It could also allow the identification of sub-

snow terrain features in areas where snow cover is present during much of the year.

The very high radar returns from old snow or firn as described by Waite and MacDonald (35) indicates the possibility of mapping firn fields using SLAR. Such mapping ability could provide information necessary to make fairly accurate estimates of a glacier's mass balance. One method of achieving this estimate is by noting the position of the firn line which separates firn above and glacial ice below on a glacier at the end of the ablation season. The yearly movement of this line either up or down the glacier could tell whether the mass balance is negative or positive respectively (36). Another method of mass balance estimation which is also described by LaChappelle is the use of the accumulation area ratio as defined by Meier (37). This ratio is equal to the area of snow cover at the end of the ablation season (= firn) within a given locality divided by the total area of glacial ice present. Changes in this ratio can signify changes in glacier mass balance and also weather conditions.

The amount of melt water present on, near and downstream from a glacier is also an important indicator of its mass balance, especially the negative portion. Water has a very distinctive low return on SLAR imagery that allows it to be easily mapped in most situations.

The appearance of glacial ice on SLAR as described in the publications reviewed varied considerably from fairly bright, fine textured tones on the X-band imagery studied by Page to widely varying tones on the Ka-band imagery of Leighty to generally dark tones on imagery analyzed by Waite and MacDonald, also Ka-band. The ability to recognize glacial ice is essential to its study with SLAR since the mapping of glaciers on a world-wide basis would be an important objective with an orbital system. The location of the margins of glaciers and the movement of those margins with time are important indicators of glacial activity and possibly climatic changes as well. The shape of the glacial margin is also important, LaChappelle (36) has shown that an advancing

glacier usually has a steep or vertical front, a retreating glacier has a gently sloping front and a glacier in equilibrium has a front with a moderate slope. The identification and monitoring of crevasses in glaciers can provide information on structural glaciology and relative rates of flow in glacial ice as extracted by Leighty in Greenland. This information can in turn allow the inference of subglacial topography due to the deformation it induces in overflowing glacial ice.

Ideally, SLAR should be able to penetrate ephemeral snow; distinguish between firn, glacial ice, water, and land; and provide information on the surface features of glaciers. To some extent, SLAR can do all of these things right now; however, studies should be conducted to determine how well it does them, what surface conditions influence radar performance, and what system parameters could give optimum results. A year long study of both a temperate and polar type glacier by multifrequency and possibly multipolarized imaging radars assisted by simultaneous ground truth collection, could provide answers to these questions. Ground truth should include air and snow and ice temperatures, snow depth, the density, size, and water contents of snow, firn, and glacial ice, and depth to glacial ice. Experiments should be performed several times in the course of a year to determine the effects that increasing snow depth, physical changes in snow and ice, and the onset and progression of ablation have on radar imagery of glacial environments.

3. MISSION REQUIREMENTS

A brief study has been made of mission requirements using simplified orbital considerations. Many of the mission requirements cannot be adequately defined without further research, and this is indicated where it applies. The most difficult requirement to meet is that for repetition at very close intervals. Daily repetition with a single satellite is almost impossible even at high latitudes, but a properly designed system may be able to give adequate coverage on a two-day basis, as shown.

3.1 Angle of Incidence Requirements

Little is known about the true requirements for angle of incidence to be used in polar missions, as shown in Table 3.1-1. Enough measurements have been made of sea ice, however, so that we know that relatively large angles of incidence are effective and near-vertical incidence is less effective.

TABLE 3.1-1 Angle of Incidence Requirements
for Polar Missions

Sea Ice	$25^{\circ} < \theta < \text{TBD}$ (60° works well)
Icebergs	TBD (Larger angles probably better)
Glaciers and Continental Ice	TBD (May depend upon setting)

As stated in Section 2.1, the only quantitative measurements of backscatter from sea ice have been made with the 13.3 GHz and 0.4 GHz NASA/JSC scatterometers. These systems operate out to about 60° , and the sensitivity to sea-ice differences seems to increase with increasing angle, although there is little difference between the responses in the 30° - 60° range. Below about 25° the ability to discriminate is nearly lost. Imaging radars that have been used in sea-ice studies normally operate with angles of incidence well beyond 60° , but direct comparison has been made between their capabilities and the smaller-angle capabilities; hence, we must consider the outer edge of the range of useful angles undefined until further research has been performed.

No information is available at all on the effect of angle of incidence variations on radar return from icebergs. However, knowledge of the physics of radar returns permits drawing the conclusion that larger angles of incidence will probably be superior to smaller angles. The radar backscatter from the sea around the icebergs, and to a lesser extent from the ice around bergs embedded in the pack, is smaller at larger angles of incidence, whereas the return from the edge of a berg should be enhanced because of corner reflector effects at its edges--at least for steep-sided varieties. Thus the berg signal-to-clutter ratio should be better at larger angles where the clutter is smaller but the berg signal is not.

The proper angles of incidence for observing glaciers and continental ice sheets are completely unknown, and they may depend both on the purpose of the mapping and the setting of a glacier. For instance, one might expect to do better at detecting crevasses at angles near enough to vertical so that attenuation in the overlying snowpack would be minimized. On the other hand, gentle slopes and small features might be enhanced by imaging them at angles near grazing incidence. Glaciers lying in the mountains will often require an angle of incidence dictated by the direction and slopes of their surroundings; too steep an angle results in excessive "radar layover", a form of geometric distortion, and too shallow an angle results in excessive shadowing. The same criteria should apply for mapping mountain glaciers that apply for any other radar imaging in mountainous terrain, a subject that has been thoroughly investigated by geologists.

The need for research into proper angles of incidence is clear for sea ice and icebergs, and for parts of the glacier/continental-ice problem. The general subject of needed research is discussed in Section 2 and Appendices A, B, and C.

3.2 Coverage Requirements

Detailed analysis of the coverage requirements is beyond the scope of this study, for it would involve a careful study of the true requirements of a variety of potential users of the information.

Nevertheless, some indications of the coverage requirements can be derived from general knowledge of the potential applications such as that described in Section 2. Unfortunately some of the requirements call for very frequent repeat coverage, and this is difficult to achieve because of the ambiguity limitations of synthetic-aperture radar in space. This limitation can be overcome by use of the SCANSAR technique, but only at the price of degraded resolution; one cannot have both fine resolution and extended coverage without excessive power and system complexity.

TABLE 3.2-1 Coverage Requirements for Polar Missions

Sea Ice	
Navigation	1-5 days in critical areas
Meteorology	5-7 days
Icebergs	1-3 days in critical areas
Glaciers and Continental Ice	Monthly

Table 3.2-1 outlines our estimates of the coverage requirements for the different phases of a polar mission. Clearly requirements associated with navigation call for frequent mapping of the pack ice and icebergs, since both can move significantly in a relatively short period of time. Useful information about the pack ice can be obtained with somewhat less frequent coverage (say 5 days) which permits general monitoring of the movement and changes in extent of the pack, but critical areas where ships are to go through relatively narrow leads should be monitored more frequently. Perhaps the optimum remote-sensing system for navigation through the ice involves general monitoring by satellite with detailed monitoring of critical areas pointed out on the satellite images conducted by radar-equipped aircraft or, in some places, shore-mounted radar systems. Icebergs moving in well-defined currents under known wind conditions can be tracked and their future positions estimated with less-frequent coverage, but in some places and conditions this is practical only for short times. As with the pack ice, a combined satellite and aircraft system is probably called for in the most critical areas at critical times.

The total extent of open and ice-covered water is of great meteorological significance, but this does not change so rapidly that daily coverage is required. Presumably weekly coverage should be adequate for this purpose, with any gross rapid changes being detected by the wider-coverage passive microwave systems currently in use.

The repetition interval for glacier and continental-ice-sheet monitoring is not known. Certainly monthly monitoring as indicated should be frequent enough. If less frequent monitoring is needed, any system that can accomplish the other polar mission requirements can certainly handle this one.

The problem with frequent coverage is that the swath covered per orbit must be large. A simple calculation has been made assuming a "perfect" polar orbit in which each track is separated from its adjacent tracks by just the amount of the earth's rotation during an orbit. Computations were made for 50° and 60° latitudes. 50° latitude would cover most of the areas (but not all) where icebergs are a problem and nearly all of the areas of significant pack-ice cover except the St. Lawrence River estuary and part of the Sea of Okhotsk. The 60° latitude covers most of the pack-ice regions during the majority of the year, but misses a significant amount of the iceberg area south of Greenland. Swath widths required under these conditions are shown in Table 3.2-2.

TABLE 3.2-2 Swath Widths Required for Repeat Coverage-Perfect Polar Orbit-Simplified Calculations

Repetition Interval (days)	Swath for Daytime Only 50° Latitude (km)	Swath for Daytime Only 60° Latitude (km)	Swath for Day and Night 50° Latitude (km)	Swath for Day and Night 60° Latitude (km)
1	1662	1292	831	646
2	831	646	415.5	323
3	554	277	432	216
5	332	259	166	129
7	238	185	119	92

TABLE 3.2-3 Swath Widths Possible
for One-Side Coverage

Height (km)	Swath Width in km 5 Scan Cells				Swath Width in km 10 Scan Cells			
	Minimum Incidence Angle 20°		Minimum Incidence Angle 30°		Minimum Incidence Angle 20°		Minimum Incidence Angle 30°	
	Safety Factor	Safety Factor	Safety Factor	Safety Factor	Safety Factor	Safety Factor	Safety Factor	Safety Factor
	2	1.5	2	1.5	2	1.5	2	1.5
500	188	269	163	247	279	383	257	374
1000	217	344	187	279	350	492	308	466

Two sets of swath widths are shown for each latitude: "day-time only" representing one coverage per orbit and "day and night" representing coverage on both the ascending and descending parts of each orbit. Presumably the latter would be the mode selected for a polar satellite, since the swath required in the "daytime only" mode is too great and there is no particular reason that the radar should operate only during daytime--which does not really exist at all during the polar winter anyway. As shown below, the daily coverage does not appear feasible, but 2-day coverage looks possible, and weekly coverage is easy. Of course, these coverages are for the latitudes shown, and coverage will be better at the higher latitudes.

Appendix D discusses the coverage considerations for a SCANSAR operating at angles of incidence appropriate to a polar mission. Some significant conclusions for this purpose are summarized in Table 3.2-3. Ideally one would like to operate at angles of incidence of 30° or beyond for the polar mission, as nearly as can be determined at this time. On the other hand, the swath width possible when operation is allowed in to 20° incidence is greater, and some compromise might have to be made, so both are shown to give an idea of the gain to be expected from compromising the angle-of-incidence requirements.

A system using 5 scan cells will be simpler to build than one using 10 scan cells, for the former antenna may be feasible with a switching matrix to perform the scanning, whereas the latter will surely require use of programmed phase shifters. Achieving 50° 2-day coverage will require use of 10 scan cells, but one possible configuration with 20° incidence permitted would permit 60° 2-day coverage with 5 scan cells.

The factor of safety used in accounting for the fall-off of the antenna pattern outside the main beam makes a big difference in the achievable swath. The simplest antenna illuminations require larger factors of safety, but a factor of safety of 1.5, the minimum indicated, may well be feasible if a suitable illumination distribution is used in the antenna. This should be feasible in the along-track dimension (at the expense of using a longer antenna than the effective 10 meters indicated), but it will be more difficult in the across-track direction where scanning must take place. Perhaps a compromise solution involving a carefully designed distribution in the along-track direction with a 1.5 safety factor and a simpler distribution in the across-track direction with a 2 safety factor might be the best arrangement. At any rate, these factors must be considered in evaluating the tradeoffs between complexity, cost, and coverage for a polar SCANSAR.

3.3 Polarization Requirements

As indicated in Section 2.1, the best discrimination of sea-ice types and thickness is achieved with cross polarization. Present knowledge indicates that there is little distinction between the like polarizations, although this is based on meager information and might change after further research. The problem with use of cross-polarized signals is that they are weaker than like-polarized signals so more power is required of the radar to achieve adequate signal-to-noise ratio. Thus, although cross polarization is the most desirable mode, a like-polarized mode may be forced by power limitations. This, and other polarization considerations, is indicated in Table 3.3-1.

TABLE 3.3-1 Required Polarizations

Sea Ice	VV or HH acceptable, Cross (VH or HV) preferred.
Icebergs	TBD (HHor cross probably better)
Glaciers and Continental Ice	TBD

No information is available on the best polarization for detecting icebergs. However, radar backscatter from the sea, at least at low wind speeds, is less for horizontal than for vertical polarization. Since there is no reason to suspect that the icebergs themselves will give lower horizontally polarized returns, the use of horizontal polarization is indicated for the best signal-to-clutter ratio.

So little information is available on radar return from glaciers and continental ice sheets that nothing can be said about an optimum polarization. Probably there will be little choice between vertical and horizontal polarizations, and cross-polarization will probably be a useful adjunct as it is in other land imaging--but these are just speculations in lieu of the needed research.

3.4 Resolution Requirements

Table 3.4-1 summarizes the unfortunate state of our knowledge of required resolutions. In reality, true resolution requirements have not been determined for any radar imaging application; and those applications in the polar mission are no exception!

TABLE 3.4-1 Required Resolutions

Sea Ice	
Navigation	TBD
Meteorology	TBD (Probably larger than for navigation)
Icebergs	TBD
Glaciers and Continental Ice	TBD

For sea ice, although the resolution requirement is unknown, the resolutions that have been used in some of the experiments are known. Resolutions of 10 m or so were used in the Johnson and Farmer work with the NRL 4-frequency-radar discussed in Section 2.1. The NASA and Coast Guard AN/DPD-2 radar systems used in Parashar's work and the experiment in connection with the Northwest Passage transit of the tanker Manhattan had a resolution of the order of 15 meters. Most of the more recent work has used the AN/APS-94 with a pixel of some 75 x 100 to 75 x 300 m, and this system has also been used in the Great Lakes experiment by NASA Lewis RC. All of these experiments have been successful to a degree, but none of the data has been analyzed to illustrate the actual required resolution for different portions of the sea-ice monitoring task. The success of the AN/APS-94 experiments, however, seems to indicate that truly fine resolution is not required for sea-ice monitoring even for navigation. Because of this, the study in Appendix D was conducted using a nominal 50 m resolution, but the 100 m resolution required to achieve 10 scan cells with 2 independent looks each seems not to be out of the question.

The resolution required for iceberg monitoring is also an open question. Most radar iceberg surveys, as indicated in Section 2.2, have been with shore-based or ship-based PPI radars that have very poor resolution. On the other hand, some of the problems encountered may have been due to this poor resolution. The question that must be determined is whether the resolution must be adequate to resolve parts of the icebergs to distinguish them from ships or whether it is sufficient to detect icebergs--which would call for a much poorer resolution. Furthermore, the user community must define the minimum size of iceberg to be detected and possibly resolved.

No information is available about the resolution required in the glacier and continental ice sheet problem. Intuitively, one would expect that small glaciers would require better resolution than continental ice sheets, but this calls for an experiment to verify this conclusion, as well as extensive discussions with potential users.

The methodology for determining resolution requirements has been established (Moore, 1976). Controlled experiments are now needed using this methodology on images of ice in its various forms.

REFERENCES

1. Thorndike, A. S. and G. A. Maykut, "On the Thickness Distribution of Sea Ice," AIDJEX Bulletin No. 21, pp. 31-48, Division of Marine Resources, University of Washington, 1973.
2. Koerner, R. M., "The Massbalance of the Sea Ice of the Arctic Ocean," Journal of Glaciology, vol. 12, No. 65, pp. 173-185, 1973.
3. Ackley, S., W. Hibler, III, F. Kugzruk, A. Kovacs and W. Weeks, "Thickness and Roughness Variations of Arctic Multi-year Sea Ice," AIDJEX Bulletin No. 25, July, 1974.
4. Groen, P., The Waters of the Sea, D. Van Nostrand Co. Ltd., London, 1967.
5. Weeks, W. F. and A. Assur, "Fracture of Lake and Sea Ice," Research Report 269, Cold Regions Research and Engineering Laboratory, Hanover, New Hampshire, September, 1969.
6. Anderson, V. H., "Sea Ice Pressure Ridge Study: An Airphoto Analysis," Photogrammetria, Elsevier Publishing Company, Amsterdam, 1970.
7. Kazo, Thomas L. and Orest I. Diachok, "Spatial Variability of Topside and Bottomside Ice Roughness and its Relevance to Underside Acoustic Reflection Loss," AIDJEX Bulletin No. 19, March, 1973, Arctic Ice Dynamics Joint Experiment, Division of Marine Resources, University of Washington, Seattle, Washington 98105.
8. Ling, Chi-Hai and Norbert Untersteiner, "On the Calculation of the Roughness Parameter of Sea Ice," AIDJEX Bulletin No. 23, January, 1974.
9. Hoekstra, P. and P. Cappillino, "Dielectric Properties of Sea Ice and Sodium Chloride Ice at UHF and Micro-Wave Frequencies," Journal of Geophysical Research, vol. 76, no. 20, pp. 4922-4931, July, 1971.
10. Anderson, V. H., "High Altitude, Side Looking Radar Images of Sea Ice in the Arctic," Proceedings Fourth Symposium on Remote Sensing of Environment, University of Michigan, Ann Arbor, pp. 845-857, June, 1966.
11. Bradie, R. A., "SLAR Imagery for Sea Ice Studies," Photogrammetria Engineering, vol. 33, no. 7, 1967.
12. Johnson, J. D. and L. D. Farmer, "Use of Side-Looking Airborne Radar for Sea Ice Identification," Journal of Geophysical Research, vol. 76, no. 9, pp. 2138-2155, March, 1971.

13. Johnson, J. D. and L. D. Farmer, "Determination of Sea Ice Drift Using Side-Looking Airborne Radar," Proceedings 7th International Symposium on Remote Sensing of Environment, The University of Michigan, Ann Arbor, 1971.
14. Biache, A., Jr., C. A. Bay and R. Bradie, "Remote Sensing of the Arctic Ice Environment," 7th International Symposium on Remote Sensing of Environment, Proceedings, University of Michigan, Ann Arbor, vol. 1, 1971.
15. Ketchum, R. D., Jr. and S. J. Tooma, Jr., "Analysis and Interpretation of Airborne Multi-Frequency Side-Looking Radar Sea Ice Imagery," Journal of Geophysical Research, 78C37, pp. 520-538, 1973.
16. United States Coast Guard, "Data Reduction of Airborne Sensor Recrods," Report No. DOT-CT-01-800-A, Department of Transportation, Office of Research and Development, Washington, D. C. 20591, July, 1970.
17. United States Coast Guard, "Analysis of SLAR Imagery of Arctic and and Lake Ice," Report No. DOT-CG-14486-A, Department of Transportation, Office of Research and Development, Washington, D. C. 20591, March, 1972.
18. United States Coast Guard, "Interpretation of Winter Ice Conditions from SLAR Imagery," Report No. DOT-CT-14486-1A, Department of Transportation, Office of Research and Development, Washington, D. C. 20591, February, 1972.
19. Glushkov, V. M. and V. B. Komarov, "Side-Looking Imaging Radar System TOROS and Its Application to the Study of Ice Conditions and Geological Explorations," Proceedings 7th International Symposium on Remote Sensing of Environment, University of Michigan, Ann Arbor, 1971.
20. Loshchilov, V. S. and V. A. Voyevodin, "Determination of Elements of Ice Cap Drift and Movement of Ice Edges by Means of the Airborne Side-Scan Radar 'TOROS'," Problems in Arctic and Antarctica, vol. 40, pp. 23-30, 1972.
21. Zagorodnikov, A. A., V. S. Loshchilov, and K. B. Chelyshev, "Two-Dimensional Statistic Analysis of Radar Imagery of Sea Ice," 8th International Proceedings, University of Michigan, Ann Arbor, vol. 1, 1972.
22. Moore, R. K., report on trip to USSR, June, 1973 (unpublished memorandum).
23. Canadian Department of Atmospheric Environment, "Operation Ice Map II, Side-Looking Radar Trials," 1972.
24. Moore, R. K., "Radar Scatterometry - An Active Remote Sensing Tool," University of Kansas Center for Research, Inc., CRES Technical Report 61-11, Remote Sensing Laboratory, Lawrence, Kansas, April, 1966.

25. Rouse, J. W., Jr., "Arctic Ice Type Identification by Radar," University of Kansas Center for Research, Inc., CRES Technical Report 121-1, Remote Sensing Laboratory, Lawrence, Kansas, August, 1968.
26. Parashar, S. K., "Investigation of Radar Discrimination of Sea Ice," (Ph.D. Dissertation), University of Kansas Center for Research, Inc., CRES Technical Report 185-13, 1974.
27. Personal Communication with N. de Villiers of Canadian Center for Remote Sensing, 1974.
28. Cummings, W.A., "The Dielectric Properties of Ice and Snow at 3.2 cm.," Journal of Applied Physics, vol. 23, no. 7, pp. 768-773, 1952.
29. Evans, S., "Dielectric Properties of Ice and Snow - A Review," Journal of Glaciology, vol. 5, pp. 773-792, 1965.
30. Meier, M.F., W.J. Campbell, and R.H. Alexander, 1966, "Multispectral Sensing Tests at South Cascade Glacier, Washington," in Fourth Symposium on Remote Sensing of Environment, Proceedings, Univ. Michigan, Ann Arbor, pp. 145-160.
31. MacDonald, H.C. and W.P. Waite, 1971, "Optimum Radar Depression Angles for Geological Analysis," Modern Geology, vol. 2, no. 3, pp. 179-193.
32. Leighty, R.D., 1966, "Terrain Information from High Altitude Side-Looking Radar Imagery on an Arctic Area," in Fourth Symposium on Remote Sensing of Environment, Proceedings, Univ. Michigan, Ann Arbor, pp. 575-597.
33. Page, D.F., 1975, "Application of Radar Techniques to Ice and Snow Studies," Journal of Glaciology, vol. 15, no. 73, in Symposium on Remote Sensing in Glaciology, Proc., Cambridge, England, pp. 171-192.
34. Elachi, C. and W.E. Brown, Jr., 1975, "Imaging and Sounding of Ice Fields with Airborne Coherent Radar," Journal of Geophysical Research, vol. 80, no. 8, pp 1113-1119.
35. Waite, W.P. and H.C. MacDonald, 1970, "Snowfield Mapping with K-band Radar," Remote Sensing of Environment, vol. 1, pp. 143-150.
36. La Chappelle, E., 1962, "Assessing Glacier Mass Balance By Reconnaissance Aerial Photography," Journal of Glaciology, vol. 4, no. 33, pp. 290-291.
37. Meier, M.F., 1962, "Proposed Definitives for Glacier Mass Budget Terms," Journal of Glaciology, vol 4, no. 33, pp. 252-265.

CRINC LABORATORIES

Chemical Engineering Low Temperature Laboratory

Remote Sensing Laboratory

Flight Research Laboratory

Chemical Engineering Heat Transfer Laboratory

Nuclear Engineering Laboratory

Environmental Health Engineering Laboratory

Information Processing Laboratory

Water Resources Institute

Technical Transfer Laboratory

Air Pollution Laboratory

Satellite Applications Laboratory

CRINC

